

Cross-Chain Arbitrage: The Next Frontier of MEV in Decentralized Finance

Burak Öz

Technical University of Munich &
Flashbots
Munich, Germany
burak.oez@tum.de

Bruno Mazorra

Flashbots
Barcelona, Spain
bruno@flashbots.net

Christof Ferreira Torres

Instituto Superior Técnico &
University of Lisbon & INESC-ID
Lisbon, Portugal
christof.torres@tecnico.ulisboa.pt

Jonas Gebele

Technical University of Munich
Munich, Germany
jonas.gebele@tum.de

Florian Matthes

Technical University of Munich
Munich, Germany
matthes@tum.de

Christoph Schlegel

Flashbots
Zurich, Switzerland
christoph@flashbots.net

Filip Rezabek

Technical University of Munich
Munich, Germany
rezabek@net.in.tum.de

Abstract

Decentralized finance (DeFi) markets spread across Layer-1 (L1) and Layer-2 (L2) blockchains rely on arbitrage to keep prices aligned. Today most price gaps are closed against centralized exchanges (CEXes), whose deep liquidity and fast execution make them the primary venue for price discovery. As trading volume migrates on-chain, cross-chain arbitrage between decentralized exchanges (DEXes) will become the canonical mechanism for price alignment. Yet, despite its importance to DeFi—and the on-chain transparency making real activity tractable in a way CEX-to-DEX arbitrage is not—existing research remains confined to conceptual overviews and hypothetical opportunity analyses.

We study cross-chain arbitrage with a profit-cost model and a year-long measurement. The model shows that opportunity frequency, bridging time, and token depreciation determine whether inventory- or bridge-based execution is more profitable. Empirically, we analyze one year of transactions (September 2023 - August 2024) across nine blockchains and identify 242,535 executed arbitrages totaling 868.64 million USD volume. Activity clusters on Ethereum-centric L1-L2 pairs, grows 5.5x over the study period, and surges—higher volume, more trades, lower fees—after the Dencun upgrade (March 13, 2024). Most trades use pre-positioned inventory (66.96%) and settle in 9s, whereas bridge-based arbitrages take 242s, underscoring the latency cost of today’s bridges. Market concentration is high: the five largest addresses execute more than half of all trades, and one alone captures almost 40% of daily volume post-Dencun. We conclude that cross-chain arbitrage fosters vertical integration, centralizing sequencing infrastructure and economic power and thereby exacerbating censorship, liveness, and finality risks; decentralizing block building and lowering entry barriers are critical to countering these threats.

Keywords

Cross-Chain Arbitrage, Decentralized Finance, Maximal Extractable Value, Blockchain Interoperability

1 Introduction

The blockchain ecosystem is inherently multi-chain. Layer-1 (L1) networks such as Ethereum supply security and decentralization, while a growing number of Layer-2s (L2s) deliver cheaper, higher-throughput execution. Nearly every chain now hosts its own Decentralized Finance (DeFi) markets, collectively processing several billion USD in daily trading volume [18]. This market fragmentation, however, means prices often diverge across chains. Restoring parity—and thus market efficiency—relies on arbitrage, a major form of Maximal Extractable Value (MEV) [19] in which traders buy low on one market and sell high on another.

Today, most price gaps are closed by arbitraging on-chain Decentralized Exchanges (DEXes) against off-chain Centralized Exchanges (CEXes) [37], whose deep liquidity, low fees, and fast execution—advantages afforded by their centralized infrastructure—make them the primary venue for price discovery. As blockchain execution improves, DeFi adoption grows, and long-tail tokens (which can be issued permissionlessly on-chain) remain unavailable on CEXes, trading volume is expected to shift to DEXes—a long standing goal of the DeFi industry. In that on-chain future, *cross-chain DEX-to-DEX arbitrage* will be the canonical mechanism for price alignment.

Cross-chain arbitrage can be executed in two main ways: (i) by keeping inventory on multiple chains or (ii) by moving assets through a bridge. Holding inventory ties up capital and exposes the trader to price swings on each chain but allows near-instant execution when an opportunity arises. Bridging avoids those inventory risks yet incurs transfer delays, exposing the opportunity to competitors who can act first or to routine trading activity that can close the price gap. Arbitrageurs must therefore choose a method based on the pairs they target and the bridges available. Figure 1 illustrates real-world examples of both methods (details in Appendix B).

Despite its importance to DeFi—and the on-chain transparency that lets us track dynamics invisible in CEX-to-DEX arbitrage—cross-chain arbitrage remains under-explored. While single-domain MEV is well documented [19, 29, 30, 51, 54, 56, 71], work on cross-chain

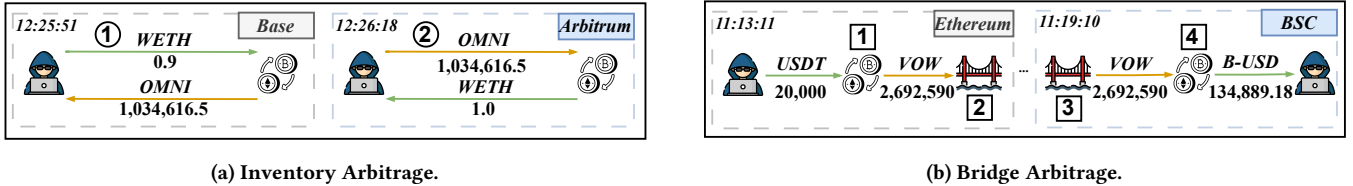


Figure 1: Cross-chain arbitrage execution methods. (a) Inventory arbitrage: the trader holds capital on both chains, so both legs can settle almost simultaneously. **(b) Bridge arbitrage:** the trader moves assets across chains between legs, and the bridge delay dominates total settlement time. Full transaction details appear in Appendix B.

arbitrage, a subset of cross-domain MEV, is sparse. Conceptual overviews of cross-domain MEV lack a domain-specific model that contrasts inventory and bridge arbitrage [42, 47]. Empirical work has either examined CEX-to-DEX arbitrage by observing only the on-chain leg [37] or studied hypothetical, inventory-based cross-chain opportunities limited to a few market pairs [35, 39].

We close this gap by combining a profit-cost model for cross-chain arbitrage—which determines when to bridge versus hold inventory—with a year-long empirical study on executed arbitrages across nine blockchains.

Contributions. We make the following contributions:

- We present a profit-cost model that compares inventory and bridge cross-chain arbitrage, accounting for the costs of non-instantaneous bridging and holding inventory. The model solution reveals opportunity frequency, bridging time, and token depreciation as key determinants.
- We develop a general methodology for (i) detecting executed cross-chain arbitrages and (ii) classifying the bridge transactions that link their two legs.
- We conduct the first large-scale study of executed cross-chain arbitrages—242,535 trades totaling 868.64 million USD volume across nine blockchains—revealing activity concentrated on Ethereum-centric L1-L2 pairs, growing by 5.5× over the study period and spiking (higher volume, more trades, lower fees) after the Dencun upgrade (March 13, 2024).
- We show that most arbitrage (66.96 %) relies on pre-positioned inventory rather than bridges, settling in a 9 s median, whereas bridge-based trades take 242 s, highlighting the latency cost of today’s bridges.
- We uncover rising market concentration: five largest addresses generate over half of all trades, and one alone (0xCA74) captures up to 40 % of daily volume in the post-Dencun period.
- We point that cross-chain arbitrage encourages vertical integration, concentrating sequencing infrastructure and economic power and thereby heightening censorship, liveliness, and finality risks; we outline decentralizing block building and lowering entry barriers as countermeasures.

2 Background

This section provides relevant background on DeFi, MEV, L1 and scaling solutions, and blockchain interoperability and bridges.

2.1 Decentralized Finance

DeFi offers similar primitives as Traditional Finance (TradFi) but extends it via additional solutions that are solely enabled by blockchain technology. These include DEXes, lending platforms, options markets, and tokenized assets, all implemented via smart contracts. While CEXes use a Central Limit Order Book (CLOB) model, which relies on a centralized entity for order matching and settlement, DEXes typically adopt Automated Market Makers (AMMs) to facilitate Peer-to-Peer (P2P) trading, although the CLOB model has also been used historically (e.g., EtherDelta).

AMMs rely on liquidity pools and deterministic pricing rules to execute trades without intermediaries. A widely used design is the Constant Product Market Maker (CPMM) adopted by Uniswap V2 [3]: for pool reserves x and y , all swaps must satisfy $x \cdot y = k$. A trade moves the reserves along this curve, setting a new price, while liquidity deposits or withdrawals change the curve (and hence k) without altering the instantaneous price.

Trading on DEXes therefore introduces price slippage—both expected, due to trade volume and liquidity constraints, and unexpected, due to execution delays and market volatility. Either form can push CPMM prices out of line with other pools or venues, creating the arbitrage opportunities that traders exploit.

2.2 Maximal Extractable Value

The decentralized infrastructure enables opportunities for MEV extraction. MEV relies on two key transaction ordering primitives: frontrunning, where an extractor ensures their transaction precedes a target transaction (T_{Target}), and backrunning, where the extractor’s transaction executes immediately after T_{Target} . Common MEV strategies include arbitrage, liquidation, and sandwiching. Arbitrage exploits price discrepancies across exchanges by analyzing blockchain state changes, ensuring price alignment across DEXes. Liquidations involve repaying a debt to purchase discounted collateral, often focusing on fixed-discount opportunities that can be executed in a single transaction. Both arbitrage and liquidation are generally considered beneficial for market efficiency. In contrast, sandwiching is a manipulative strategy where an adversarial transaction wraps a target trade (T_V), buying the asset beforehand to profit from the price increase caused by T_V , and subsequently selling at a higher price. This practice disrupts fair-price execution and is considered harmful.

Competition among MEV extractors may cause block congestion and gas fee inflation. MEV can also result in systemic instability by incentivizing behaviors prioritizing individual gain over network

security. In the context of blockchain, this can lead to consensus instabilities, as miners or validators may be incentivized to steal transactions from others by creating forks, thereby undermining the system’s integrity. Among the various strategies for MEV extraction, arbitrage is the most prevalent, as demonstrated in measurement studies in [19, 30, 54].

While MEV is typically studied on a single chain, value can also be extracted across domains. A domain is any system with a shared mutable state—L1 and L2 blockchains, CEXes. [47] formalize cross-domain MEV as the maximum cumulative balance increase a user can achieve by controlling transaction sequencing across several such domains. In this work we focus on one concrete subset: executed DEX-to-DEX arbitrage that spans multiple blockchains.

2.3 Layer-1 and Scaling Solutions

L1 refers to the classical blockchain model where transactions are recorded on a public, immutable, and trustless ledger which follows a consensus algorithm to determine block creation. Examples of popular L1s include Ethereum [68], Binance Smart Chain [13], Avalanche [55], etc. However, L1s can face scalability issues in terms of throughput and transaction fees. As a result, a number of so-called L2 scaling solutions have emerged, where the most prominent solutions are either based on sidechains (e.g., Polygon [23]) or commit chains (e.g., rollups). Commit chains or rollups can be further split into either optimistic (e.g., Arbitrum [7], Base [11], Optimism [50]) or zero-knowledge based (e.g., ZKsync [73], Scroll [57]) depending on what types of proofs are used to verify the validity of L2 transactions. Sidechains typically run a fast consensus mechanism among few peers in parallel to L1. On the other hand, rollups enable throughput scaling by off-loading compute and (possibly) storage resources off-chain without a need for large-scale consensus, which is provided by the underlying L1. Generally, L2 scaling solutions allow distrustful parties to deposit funds into a bridge smart contract on L1 and then operate on L2 via L2 transactions whose state is then updated to L1.

Table 1 summarizes the various blockchains that we analyze for cross-chain arbitrage. Unlike L1s, which typically operate using a gas price model and provide public access to mempool data, L2s typically feature private mempools with transactions ordered by centralized sequencers, which often follow a First-Come, First-Served (FCFS) strategy. The latter makes it harder for users to extract MEV as they cannot observe other pending transactions nor can pay higher gas fees to prioritize their own transactions. The block time does not correspond to the finality, as L2s only offer a soft finality to its users as the transactions are only fully finalized after being settled on L1.

2.4 Blockchain Interoperability and Bridges

Blockchain interoperability aims to connect blockchain networks and transfer assets or data between them. The transfer typically involves locking assets on one chain and minting a matching representation on the destination chain, conditional on some evidence of the asset being locked. Bridges are the basic infrastructure enabling this interoperability. Using a bridge, a token can be moved from one blockchain to another while maintaining some security guarantees, with the form of guarantee depending on the means through which

Blockchain Name	Type	Mempool	Ordering	Block Time	Launch
Avalanche (AVA)	L1	Public	Gas Price	~2.00 s	Sep 2020
Binance Smart Chain (BSC)	L1	Public	Gas Price	~3.00 s	Sep 2020
Ethereum (ETH)	L1	Public	Gas Price	~12.00 s	Jul 2015
Polygon PoS (POL)	L2-SC	Public	Gas Price	~2.00 s	Jun 2020
Arbitrum (ARB)	L2-OR	Private	FCFS*	~0.25 s	Aug 2021
Base (BASE)	L2-OR	Private	Gas Price*†	~2.00 s	Aug 2023
Optimism (OP)	L2-OR	Private	Gas Price*	~2.00 s	Dec 2021
Scroll (SCROLL)	L2-ZK	Private	FCFS*	~3.50 s	Oct 2023
ZKsync Era (ZKSYNC)	L2-ZK	Private	FCFS*	~1.00 s	Mar 2023

*Centralized sequencer.

†FCFS tie-breaking.

Table 1: Overview of investigated Layer-1 (L1) and Layer-2 (L2) solutions. SC - Sidechain, OR - Optimistic Rollup, ZK - ZK-Rollup, FCFS - First-Come, First-Served.

the locking of funds is proved to minting contracts. Bridges can be categorized into either *native* or *multi-chain*. Each solution comes with different security, latency, and cost trade-offs.

Native bridges are built into the architecture of the underlying blockchain and facilitate direct transfers between their L1s and L2s. The process typically involves asset locking via a smart contract, proof generation for the locked asset, and transmission of the asset to the destination chain. On the destination chain, an equivalent amount of the asset is either minted (if the bridge uses wrapped tokens) or unlocked. These bridges often prioritize security and are tightly integrated with the chain’s architecture. Multi-chain bridges, on the other hand, are more versatile as they can support several different blockchains, while native bridges only operate between two blockchains. However, such bridges are operated by third-party companies, introducing trust assumptions for counterparty risk. Multi-chain bridges follow the same steps of locking, proof generation, and minting/unlocking on the destination chain, except that they present a unified communication mechanism that is blockchain-agnostic.

3 Theoretical Analysis

In this section, we model cross-chain arbitrage and solve it to provide theoretical results on the profitability of inventory against bridge arbitrages, and the factors impacting this decision.

3.1 Model

We model trading across two chains. On the first chain, trading happens on a CPMM with reserves R_t^A and R_t^B of the two tokens where the subscript denotes potential time dependency. On the second chain, trading happens on a perfectly liquid market where arbitrary amounts of tokens can be exchanged at a token A to token B exchange rate of Q_t . This model is a good approximation to reality, even in the case that the second market also uses a CPMM provided that the second market has more liquidity than the first market. We choose a perfectly liquid market for ease of exposition, to make the cost of inventory calculation less involved. See, however, Appendix A for a derivation of the cost of inventory in the case of a CPMM with limited liquidity in the second market.¹

¹Qualitatively, the results would be similar, with the caveat that liquidity constraints in the second market make bridging relatively more attractive than buying and maintaining inventory in the second market, which would be more costly in that case.

Token A is the numéraire for the subsequent calculations, i.e., we measure value and cost in token A . We assume that the two market, and the bridge operate without fees, and that gas and transaction costs for swaps and bridging are negligible. Moreover, we assume that the exchange rate in the second market follows a geometric Brownian motion with percentage drift μ and percentage variance σ . We assume that the risk-free rate was already subtracted so that μ is the excess return over the risk-free investment. We generically think of token B as a token with negative excess return over the risk-free investment so that $\mu < 0$. Implicitly, this means that the market is incomplete so that token B cannot, or only at high cost, be shorted. If on the other hand, $\mu > 0$, the subsequent discussion would be somehow trivial, as in that case the arbitrageur would rather want to hold token B permanently after having bought it, rather than selling it for arbitrage profits on the second market.²

We assume that arbitrage opportunities of equal size arrive according to a Poisson process with rate λ : this means that the exchange rates $P_t := R_t^A/R_t^B$ and Q_t in the two markets are the same almost always, but every λ^{-1} minutes on average, we have $P_\tau < Q_\tau = pP_\tau$ for a constant factor $p > 1$, where τ is the random arrival time of the opportunity.³ In a hypothetical world without frictions where tokens can be bridged instantaneously between the two market at zero cost or the arbitrageur can hold inventory of the second token in the second market at zero cost, a profit-maximizing arbitrageur sells an amount of

$$(\sqrt{p} - 1)R_\tau^A$$

token A in the first market to obtain an amount of

$$(1 - \sqrt{1/p})R_\tau^B$$

token B that he sells in the second market to obtain an overall profit of

$$(\sqrt{p} - 1)^2 R_\tau^A.$$

Figure 2 plots the change in arbitrage profit with respect to p . See, e.g., [34] for a derivation of the profit and optimal trade size.

3.1.1 Non-Instantaneous Bridging. Now suppose, bridging is non-instantaneous and it requires time $\Delta > 0$ to bridge funds from the first to the second market. If the arbitrageur does not hold inventory on the second market, and needs to bridge from the first to the second market to complete the arbitrage, then the above formula for the optimal trade size needs to be adjusted for the expected token price depreciation during the bridging. An expected profit-maximizing arbitrageur chooses his trade expecting that after bridging he can exchange the B tokens at an (in expectation) worse exchange rate $Q_{t+\Delta}$ rather than the instantaneous rate Q_t . Thus, he chooses to trade an amount of

$$(\sqrt{p}e^{\mu\Delta/2} - 1)R_\tau^A$$

token A , to make an expected profit⁴ of

²Alternatively, we could also have non-negative excess return, but make the trader risk averse and obtain qualitatively similar results.

³The equal size assumption on arbitrage opportunities is for tractability of the model.

⁴The expectation is at time τ (i.e., conditional on the realization of τ , R_τ and Q_τ) over the uncertain realization of $Q_{t+\Delta}$. Subsequently, we denote by subscripts the time at which we take expectation.

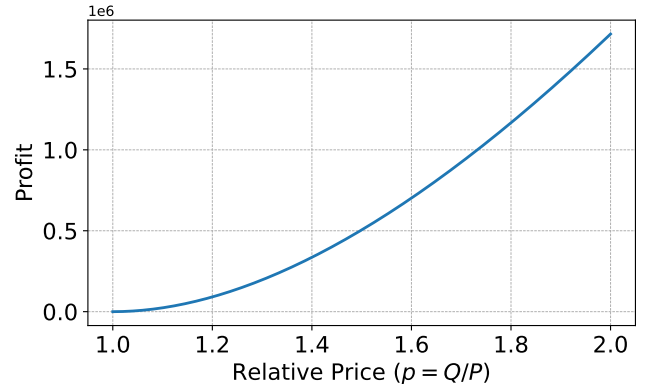


Figure 2: Arbitrage profit as a function of the relative price ($p = Q/P$) between a CPMM (P) and a perfectly liquid market (Q). Token reserve of the CPMM is fixed at $R = 10^7$.

$$\begin{aligned} & E_\tau [Q_{t+\Delta} \left(1 - \sqrt{p^{-1}} \right) R_\tau^B - (\sqrt{p} - 1) R_\tau^A] \\ &= E_\tau \left[\frac{Q_{t+\Delta}}{Q_\tau} \right] \left(1 - \sqrt{p^{-1}} e^{-\mu\Delta/2} \right) R_\tau^A - \left(\sqrt{p} e^{\mu\Delta/2} - 1 \right) R_\tau^A \\ &= \left(\sqrt{p} e^{\mu\Delta/2} - 1 \right)^2 R_\tau^A. \end{aligned}$$

Note that the expected profit is strictly smaller than in the frictionless case, as $\Delta > 0$. We call the difference in profit per unit of liquidity in the AMM,

$$C^{BR} := (\sqrt{p} - 1)^2 - (\sqrt{p} e^{\mu\Delta/2} - 1)^2,$$

the marginal cost of non-instantaneous bridging. Figure 3 illustrates the change in this cost depending on bridging time.

3.1.2 Costly Inventory. Next, we compare this to the scenario where the arbitrageur holds inventory of token B in the second market. In this case, the arbitrageur optimally needs to maintain an inventory of $I_t := (1 - \sqrt{p^{-1}})R_t^B$ units of B tokens on the second market.

The cost of inventory is given by the following expression using a standard calculation:

LEMMA 3.1. *The expected cost of inventory is*

$$C(I) := -E_0 \left[\int_0^\tau I_t dQ_t \right]$$

PROOF. Let the value of the portfolio of the arbitrageur at time t be $V_t \equiv x_t + Q_t I_t$ where x_t are his token A holdings. We use a discrete approximation and then pass to the limit: Let the time between 0 and the random arrival time τ be partitioned by $0 = t_0 < t_1 < \dots < t_n = \tau$. If the arbitrageur re-adjusts his portfolio at discrete times t_0, \dots, t_n , his token A holding change from period to period by $x_{t_i} - x_{t_{i-1}} = Q_{t_i}(I_{t_{i-1}} - I_{t_i})$. Thus, the portfolio value between re-adjustments changes by

$$\begin{aligned} V_{t_i}^{(n)} - V_{t_{i-1}}^{(n)} &= Q_{t_i} I_{t_i} + x_{t_i} - Q_{t_{i-1}} I_{t_{i-1}} - x_{t_{i-1}} \\ &= Q_{t_i} I_{t_i} - Q_{t_{i-1}} I_{t_{i-1}} + Q_{t_i}(I_{t_{i-1}} - I_{t_i}) = (Q_{t_i} - Q_{t_{i-1}}) I_{t_{i-1}}. \end{aligned}$$

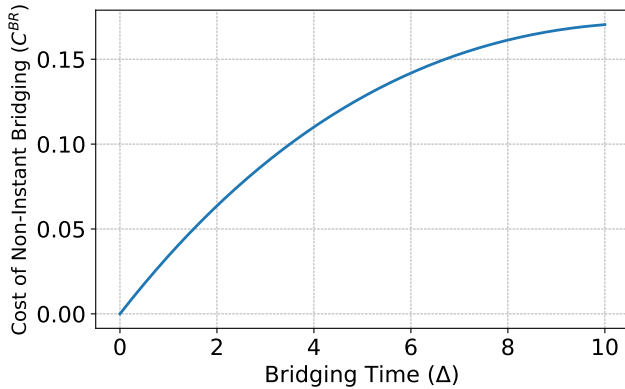


Figure 3: Cost of non-instantaneous bridging (C^{BR}) as a function of the bridging time (Δ). Parameters: relative price $p = 2$, drift $\mu = -6.25\%$.

Thus the total change in the value of his inventory over time is

$$V_0^{(n)} - V_\tau^{(n)} = \sum_{i=1}^n (V_{t_{i-1}}^{(n)} - V_{t_i}^{(n)}) = \sum_{i=1}^n (Q_{t_{i-1}} - Q_{t_i}) I_{t_{i-1}}$$

which in the limit for finer and finer partitions becomes an Ito integral

$$V_0 - V_\tau = \lim_{n \rightarrow \infty} V_0^n - V_\tau^n = - \int_0^\tau I_t dQ_t.$$

Taking expectations yields the result. \square

The cost will depend on the evolution of liquidity in the first market over time, as this determines the size of the optimal arbitrage trade. In the following, we consider the special case where the reserves take the form

$$R_t^B = \left(\frac{Q_0}{Q_t}\right)^k R_0^B$$

which gives the cost per unit traded a particularly simple form, as shown below. While the cost would take a different form in general, the class contains two reasonable and tractable cases as special case:

- (1) Liquidity in- and outflows in the AMM are such that the value of the inventory in the CPMM (in terms of token A), $R_t^A + Q_t R_t^B = 2R_t^A$, is constant. This corresponds to the case $k = 0$. This is a reasonable approximation if the time horizon considered is relatively short and the market is sufficiently liquid.
- (2) There are no inflows of liquidity so that $R_t^A R_t^B = R_0^A R_0^B$ for all $t > 0$. This corresponds to the case $k = 1/2$. This is a reasonable approximation if we are worried about an increasingly illiquid market so that the arbitrageur can make less profit from arbitraging over time.

To calculate the cost of inventory per unit traded, first note that the expected value (at time 0) of the inventory at time $0 \leq t \leq \tau$ is

$$E_0[Q_t I_t] = (1 - \sqrt{\frac{1}{p}}) R_0^A E_0\left[\frac{Q_0^{k-1}}{Q_t^{k-1}}\right] = (1 - \sqrt{\frac{1}{p}}) R_0^A e^{(k-1)(\frac{1}{2}k\sigma^2 - \mu)t}.$$

The expected cost (at time 0, i.e., with respect to the uncertain realizations of the arrival time τ and of the exchange rate changes from 0 until the arrival time τ) is given by

$$\begin{aligned} C(I) &= -E_0\left[\int_0^\tau I_t dQ_t\right] = -E_0\left[\int_0^\tau \mu Q_t I_t dt + \sigma I_t dW_t\right] \\ &= -\mu(1 - \sqrt{\frac{1}{p}}) R_0^A E\left[\int_0^\tau \frac{Q_0^{k-1}}{Q_t^{k-1}}\right] = \frac{-\mu(1 - \sqrt{\frac{1}{p}}) R_0^A}{\lambda + (1-k)(\frac{1}{2}k\sigma^2 - \mu)}. \end{aligned}$$

The expected value (at time 0) of the inventory at the time of the arbitrage τ is

$$E_0[Q_\tau I_\tau] = \frac{\lambda(1 - \sqrt{\frac{1}{p}}) R_0^A}{\lambda + (1-k)(\frac{1}{2}k\sigma^2 - \mu)}.$$

The expected cost per unit traded is therefore

$$\frac{C(I)}{E_0[Q_\tau I_\tau]} = \frac{-\mu}{\lambda}.$$

The cost is strictly positive whenever $\mu < 0$.

3.2 Results

Comparing the expected cost of bridging and the expected inventory cost at time 0, we come to the following conclusion:

THEOREM 3.2. *Let the price difference in the two markets at the time of an opportunity be $p > 1$. Define*

$$C^{BR} := (\sqrt{p} - 1)^2 - (\sqrt{p} e^{\mu \Delta / 2} - 1)^2.$$

A profit-maximizing arbitrageur chooses to hold inventory of token B if and only if

$$\frac{-\mu}{\lambda}(1 - \sqrt{\frac{1}{p}}) < C^{BR}.$$

Let us first look at the arbitrage opportunity arrival rate λ . The inequality is satisfied if and only if

$$\lambda > \frac{-\mu}{C^{BR}}(1 - \sqrt{\frac{1}{p}}).$$

Thus, if opportunities arrive frequently enough, it is worthwhile to maintain inventory. Figure 4a plots the minimum arrival rate that makes inventory profitable over bridging for each bridging time value.

Similarly, we can look at the bridging time Δ . When bridging is fast enough, it is less costly than maintaining inventory.

$$\Delta < -\frac{2}{\mu} \ln\left(\frac{\sqrt{p}}{1 + \sqrt{M}}\right), \text{ for } M := (\sqrt{p} - 1)^2 + \frac{\mu}{\lambda}(1 - \frac{1}{\sqrt{p}}).$$

Figure 4b shows, for each arrival rate, the maximum bridging delay for which bridging still outperforms holding inventory.

For low enough bridging time we can define a threshold such that for high enough expected depreciation of the value of token B the arbitrageur will bridge, while for low expected depreciation of the value of token B the arbitrageur will hold inventory.

COROLLARY 3.3. *If $1/\lambda > \Delta p$, then there is a threshold $-\hat{\mu} \leq \hat{\mu} \leq 0$ such that for low expected depreciation of the value of token B , $\mu > \hat{\mu}$, the arbitrageur chooses to hold inventory and for high expected depreciation of the value of token B , $\mu < \hat{\mu}$, the arbitrageur bridges.*

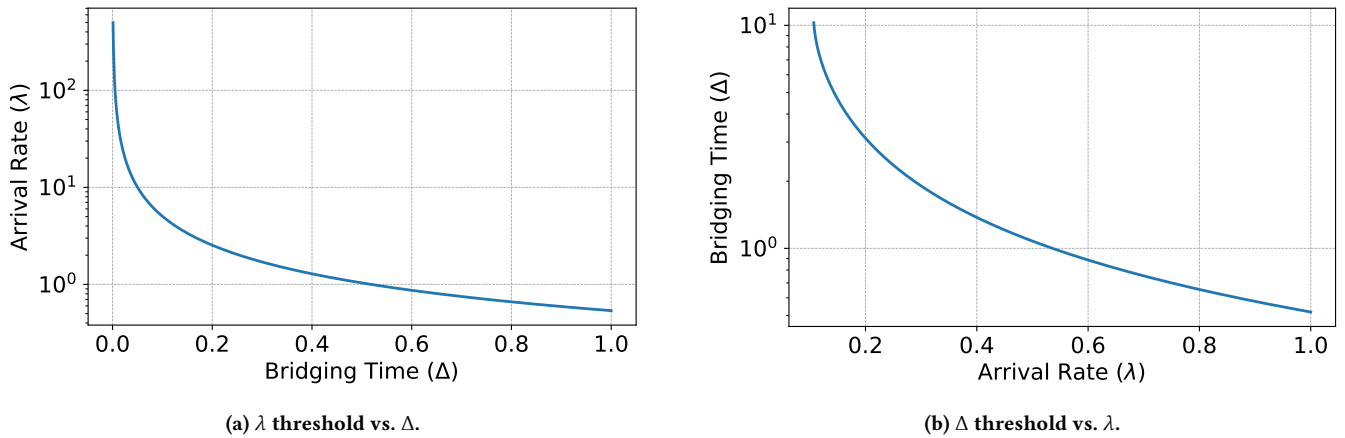


Figure 4: Profitability boundaries for inventory and bridge arbitrage as functions of bridging time (Δ) and opportunity arrival rate (λ). Parameters: relative price $p = 2$, drift $\mu = -6.25\%$. (a) Minimum λ required for inventory arbitrage to dominate as Δ varies. (b) Maximum Δ tolerable for bridge arbitrage to dominate as λ varies.

PROOF. The expression

$$\frac{-\mu}{\lambda} \left(1 - \sqrt{\frac{1}{p}}\right) - C^{BR}$$

is decreasing in μ , as can be verified from the negativity of the derivative:

$$-\frac{1}{\lambda} \left(1 - \sqrt{\frac{1}{p}}\right) + \Delta(p e^{\mu \Delta} - \sqrt{p} e^{\mu \Delta / 2}) < -\frac{1}{\lambda} \left(1 - \sqrt{\frac{1}{p}}\right) + \Delta(p - \sqrt{p}).$$

□

Figure 5 visualizes how the cost difference between inventory and bridge arbitrage changes with depreciation of the value of the token B , showing inventory becoming more costly below a threshold value.

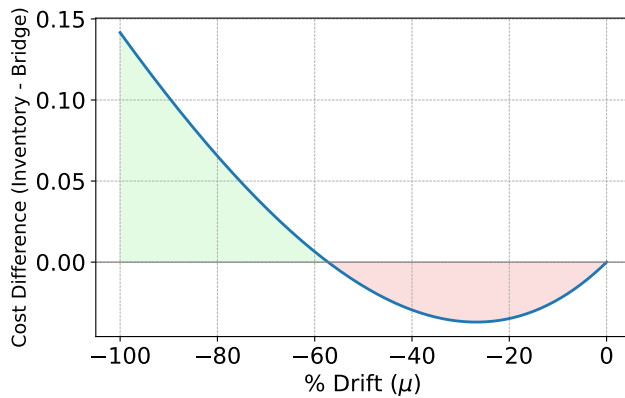


Figure 5: Cost difference (inventory – bridge) versus asset drift (μ). Positive values (green) mean bridging is cheaper; negative values (red) mean holding inventory is cheaper. Parameters: relative price $p = 2$, opportunity arrival rate $\lambda = 1$, bridging time $\Delta = 1$.

4 Empirical Analysis

In this section, we analyze a full year of executed cross-chain arbitrages across nine blockchains. After outlining our detection methodology, we describe the curated datasets and then examine the results to gauge how prevalent these arbitrages are in practice.

4.1 Detecting Cross-Chain Arbitrage

Existing arbitrage detection methods either target atomic strategies confined to a single chain [30, 41, 54, 66] or on non-atomic arbitrage between CEXes and DEXes [37]. However, neither is sufficient for cross-chain scenarios. We therefore introduce a hybrid approach that combines their key aspects.

Similar to atomic arbitrage, we require a closed cycle of trades that starts and ends with economically equivalent assets (e.g., native, wrapped, or bridged versions of the same token), such as USDC and USDT or ETH and WETH, where each trade’s output becomes next trade’s input, and the final output exceeds the initial input. Unlike atomic arbitrage, these trades span multiple transactions across different blockchains. Consequently, as with CEX-to-DEX arbitrage, single transactions may appear unprofitable in isolation but reveal profit when matched with a counterpart on another domain.

To detect such arbitrages, we focus on two-hop cross-chain cycles. Let $S_i \subseteq T_i$ denote the set of swap-event emitting transactions on blockchain i for $i \in \{1, \dots, B\}$. For any transaction pair (t_1^i, t_2^j) with $t_1^i \in S_i$, $t_2^j \in S_j$, and $i \neq j$, assume each transaction has

$$(a_{in}, x_{in}) \longrightarrow (a_{out}, x_{out}),$$

where a is the asset and x the amount. We classify the pair as a cross-chain arbitrage if it satisfies the following heuristics:

H1 Cyclic: the input and output assets of the transactions form a closed loop, $a_{out}^{t_1^i} \equiv a_{in}^{t_2^j}$ and $a_{out}^{t_2^j} \equiv a_{in}^{t_1^i}$.

H2 Marginal match: the intermediate amounts differ by at most

$$0.5\%, \frac{|x_{out}^{t_1^i} - x_{in}^{t_2^j}|}{x_{out}^{t_1^i}} \leq 0.005.$$

H3 Temporal window: the gap between t_1^i and t_2^j is ≤ 12 s for stablecoin-native pairs and ≤ 1 h otherwise.

H4 Entity link: the same Externally Owned Account (EOA) submits both transactions, or both first interact with the same MEV contract.

H1 follows the standard cycle heuristic for detecting arbitrage, except that our swaps span two transactions. We match only the input and output assets of those transactions, ignoring any intermediate swap assets. The matched assets need not be identical but must be economically equivalent.

H2 verifies that the matched swaps differ by no more than a small margin, ensuring the arbitrageur’s inventory position is unchanged aside from the final profit. For accurate accounting, we aggregate the total amounts of the original input and output assets across all swaps within a transaction. This is particularly important when trades are split into many smaller swaps, as is common with aggregator protocols that optimize execution price.

We set the marginal-difference threshold to 0.5% to account for small discrepancies from bridging fees or inventory adjustments. Sampling one hour of trades on seven different days, we compared thresholds of 1.0%, 0.5%, and 0.1%. Tightening the cut-off from 1.0% to 0.5% eliminated about 9% false positives without losing genuine matches. Reducing it further to 0.1% discarded roughly 15% valid arbitrages, proving too strict. Thus, 0.5% strikes an optimal balance, keeping true arbitrages while filtering spurious ones.

H3 captures the time-sensitive nature of cross-chain arbitrage, with a focus on the temporal window between the trades. As with other strategies, arbitrageurs must execute fast to avoid being frontrun or displaced by noise trades that erase the price gap. For stablecoin-native pairs (e.g., WETH-USDC) we impose a 12 s limit, equal to the longest block time in our dataset (Ethereum). This strict bound is justified as such pairs are typically arbitrated against continuously running CEXes [37], making longer cross-chain execution implausible. For all other pairs we allow up to 1 h, which is more of an upper bound to limit computational work. Empirically, this bound is non-restrictive: ~79% of matches occur within 10 minutes, and ~94% within 30 minutes, ensuring coverage without introducing spurious links.

H4 links the two transactions to the same actor to prevent matching unrelated trades that merely share similar assets, amounts, and timing. Specifically, the two transactions must either originate from the same EOA or both first interact with the same MEV contract. All contract addresses are cross-checked against a curated list of non-MEV contracts to avoid false positives.

After applying **H1-H4**, some transactions still appear in multiple candidate pairs. We de-duplicate using a three-level ranking:

- (1) *Marginal difference* below 0.1%. Sensitivity tests on a 70-day sample showed consistent and stable results within the range [0.001%, 0.1%]. Looser thresholds occasionally prioritized false matches.

- (2) *Time gap* ≤ 240 s. This corresponds to the average LayerZero bridging time (see Table 2), one of the most widely used cross-chain messaging protocols.
- (3) Remaining candidates are ordered by ascending marginal difference, then by ascending time gap.

For each transaction, we keep only its highest-ranked match, ensuring every pair is both economically plausible and temporally coherent.

4.1.1 Identifying Bridge Usage. To determine which strategy arbitrageurs are using—inventory or bridge arbitrage—we need a method to distinguish them. From a detection standpoint, our heuristics flag both types as cross-chain arbitrage. However, the key difference lies in the need for asset transfers: bridge arbitrage requires moving assets across chains, whereas inventory arbitrage does not. Therefore, by identifying whether bridge transactions occurred between the swaps, we can classify a cross-chain arbitrage.

Arbitrageurs typically use two types of bridges: native and multi-chain. Table 2 summarizes the bridges identified in this study, including their type, average bridging time, and detection method. Some, like LayerZero and Stargate, also serve as infrastructure for other bridges. We use two distinct approaches to detect and link bridge transactions within cross-chain arbitrages: *unique identifier* and *token transfer*.

Unique Identifier. This method utilizes unique identifiers emitted by native bridges during cross-chain transactions, enabling us to link transfers even when sender and receiver addresses differ. Detection occurs in two phases: first, we compile a dataset of all native bridge transactions within the study period; then, we examine whether arbitrageurs used these native bridges between the legs of their arbitrage.

In the first phase, we adapt the method from [30] to link native bridge transactions across Arbitrum, Base, Optimism, Scroll, and ZKSync. We construct the dataset by scanning Ethereum and the corresponding rollups for events emitted by their native bridge contracts. For instance, on Arbitrum, we match Ethereum’s *InboxMessageDelivered* event with Arbitrum’s *RedeemScheduled* event, linking transactions via the “message number”—a unique sequential ID generated by Arbitrum’s bridge contract.

Bridge Name	Bridge Type	Bridging Time	Detection Method
Across [2]	Multi-chain	1-4 mins	Token Transfer
Arbitrum One [8]	Native	15-30 mins	Unique Identifier
Axelar [9]	Multi-chain	up to 1 hour	Token Transfer
Base [59]	Native	~10 mins	Unique Identifier
Celer [15]	Multi-chain	5-20 mins	Token Transfer
LayerZero [38]	Multi-chain	~4 mins	Token Transfer
Optimism [49]	Native	1-3 mins	Unique Identifier
Polygon [24]	Native	10-30 mins	Token Transfer
Scroll [58]	Native	~4 hours	Unique Identifier
Stargate [38]	Multi-chain	~4 mins	Token Transfer
Synapse [60]	Multi-chain	10-20 mins	Token Transfer
Wormhole [69]	Multi-chain	up 24 hours	Token Transfer
ZKsync [72]	Native	~15 mins	Unique Identifier

Table 2: Overview of detected native and multi-chain bridges.

In the second phase, we examine whether a pair of native bridge transactions matches the address involved in the cross-chain arbitrage and falls within its time window. These transactions must also involve the same token used as the output of the first swap and the input of the second. If these conditions are met, we classify the arbitrage as bridge arbitrage; otherwise, as inventory arbitrage.

Note that we only consider native bridge transactions from Ethereum to rollups—not the other way around. This is because bridging to rollups typically takes a few minutes, while bridging back to Ethereum can take several days, making it impractical for cross-chain arbitrage due to the likely disappearance of price discrepancies over such a long period. Also note that the unique identifier method cannot be applied to Polygon, as its native bridge does not emit identifiable markers. For Polygon and multi-chain bridges, we instead rely on the token transfer-based method.

Token Transfer. This method links bridge transactions using ERC-20 token transfer events generated during the locking and minting process on either side of the bridge. While less precise than the unique identifier approach, it is more broadly applicable—especially for bridges that do not emit unique identifiers. We search for token transfers occurring between the two legs of an arbitrage and link them based on matching sender and receiver addresses involved in the detected cross-chain arbitrage.

We begin by scanning the source chain—where the first arbitrage leg occurs—block by block for transfer events involving the token last swapped in that leg. The search ends when we find a transfer where the sender matches the address that received the swapped tokens. On the destination chain—where the second arbitrage leg takes place—we perform a reverse block-by-block search, starting from the second leg’s block and moving backward. We look for transfer events involving the token first swapped in this leg, stopping when the recipient matches the address that initiated the second swap.

If matching token transfer events are found on both chains, as defined by the criteria above, we consider them part of the same bridge transaction. We then label the corresponding arbitrage as bridge arbitrage; if no such match is found, we classify it as inventory arbitrage.

4.1.2 Profit Calculation. For each matched transaction pair, we compute the *net profit* in USD as

$$\text{NetProfit} = (\text{USD}_{\text{out}, \text{leg 2}} - \text{USD}_{\text{in}, \text{leg 1}}) - \text{Costs}, \quad (1)$$

where **Costs** comprise

- (1) gas fees for both swap transactions,
- (2) any direct coinbase tips to the block builder⁵,
- (3) and, when present, bridge fees. (Only the source-chain call is user-initiated; the bridge operator typically submits the destination-chain leg.)

Gross revenue is simply the USD difference between the output asset of the second swap and the input asset of the first swap; subtracting the costs yields the net profit.

4.2 Datasets

We now describe the datasets we curated for our empirical analyses.

⁵A coinbase transfer is an explicit ETH payment sent to the block’s coinbase address.

4.2.1 Trading and Price Data. We processed more than 530 million trade transactions executed on nine blockchains over one year. Querying each chain via its own Remote Procedure Call (RPC) would be prohibitively costly, so we relied on Allium [5], which provides transaction-level blockchain data. From Allium, we extracted swap and aggregator protocol events. Detecting swap events across multiple blockchains is inherently challenging due to the diversity of DEXes and aggregators, many of which use non-standard event signatures. Allium’s protocol tagging revealed 104 distinct protocols involved in the cross-chain matches, giving broad coverage. For every trade, we also collected metadata such as transaction fees and, when present, direct coinbase payments. USD volumes were computed with Allium’s hourly token price model [6]. We obtained per-second ETH and BTC candlestick data from Binance [12], and used it to compute the assets’ daily price volatility.

4.2.2 Bridge Interactions. Our token transfer-based bridge detection method leverages token transfer events extracted via Allium’s raw logs dataset. As our detection method is very generic and does not reveal the specific bridging protocol used, we rely on Allium’s labeled bridge dataset to identify the underlying bridge for each transaction—something not possible through token transfers alone. However, it is important to note that Allium’s dataset covers only a subset of bridges and hence does not provide labels for all transactions.

4.2.3 Smart Contract Labels. To distinguish cross-chain arbitrage MEV bot contracts from unrelated contracts, we assembled a negative set of 1,285,481 unique addresses. Sources include DeFi protocol labels by Allium and Dune Analytics [26], known non-MEV contract lists [67], and addresses of market makers we have identified.

4.2.4 Ethereum Mempool Data. We used Mempool Dumpster dataset by Flashbots [31] to identify private Ethereum transactions. This dataset includes entries for Ethereum transactions observed by node providers in the mempool before being included in a block. Transactions missing from this dataset were likely privately relayed to Ethereum block builders through endpoints such as Flashbots Protect [32] or MEV Blocker [43].

4.3 Limitations

Our cross-chain arbitrage detection methodology identifies only two-hop cycles and relies on strict heuristics (marginal difference, temporal window, entity match), so results are a lower bound. Recently introduced DeFi or bridge protocols not tracked by Allium are missing, and Allium’s pricing model may lack data for less popular tokens, preventing USD volume estimates for those pairs. Inventory risk is not priced in arbitrage profits. Finally, Ethereum mempool data is limited by Mempool Dumpster’s network coverage.

4.4 Results

We analyze the cross-chain arbitrages detected by our methodology.

4.4.1 Cross-Chain Arbitrage Landscape. From September 2023 to August 2024, we identify 242,535 cross-chain arbitrages executed across nine blockchains. Collectively, they account for approximately 868.64 million USD in trading volume, generating 10.05 million

USD in revenue, and yield 8.65 million USD as net profit for arbitrageurs. We find that most activity (58.35 %) occurs between an L1 and L2, potentially due to the additional availability of native bridges. In contrast, L2-L2 arbitrages (35.67 %) must rely on third-party multi-chain bridges or pre-positioned inventory.

By count, Arbitrum hosts the largest share of arbitrage transactions (20.35 %). However, Ethereum dominates in volume with 36.44 % and appears in all four highest-volume arbitrated chain-pairs, which also deliver the highest profits (see Table 7 in Appendix C). Ethereum’s prominence can be attributed to the substantial liquidity available on its DEXes [22] and its central role as the settlement layer for finality of many rollups that offer native bridges.

We track daily cross-chain-arbitrage volume and each chain’s share to uncover trends. Figure 6 shows that arbitrage activity gains traction over time. We find that average daily volume grows by 5.5 \times , with a noticeable surge for Ethereum and several rollups beginning in March 2024. This jump aligns with Ethereum’s Dencun upgrade (March 13, 2024) [28], which introduced blob-carrying transactions and cut rollup transaction fees—dropping, for example, from 0.5 USD to 0.003 USD on Base [16]—and thus making rollup-based cross-chain arbitrage more attractive.

We assess Dencun’s impact on three daily aggregates—mean fee, trade count, and USD volume—using two-sided Welch t -tests (full results in Table 3). Average per-arbitrage cost falls from 6.27 USD to 4.61 USD ($t_{365} = 5.43$, $p = 1.06 \times 10^{-7}$); daily trade count rises from 548 to 788 ($t_{350} = -8.63$, $p = 2.19 \times 10^{-16}$); and volume more than doubles from 1.56 million to 3.27 million ($t_{314} = -11.9$, $p = 2.93 \times 10^{-27}$). These results show that the Dencun upgrade coincides with a clear reduction in per-trade costs and a large, statistically significant expansion in cross-chain-arbitrage activity.

Figure 6 also reveals rapid growth on Base. Besides the fee reductions via Dencun—which affect Base slightly more because

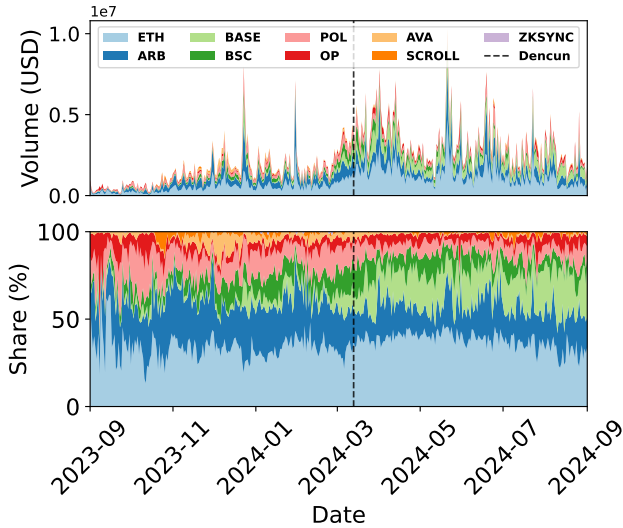


Figure 6: Daily USD cross-chain arbitrage volume (top) and per-chain share (bottom). The black dashed line marks Ethereum’s Dencun upgrade on March 13, 2024.

Metric	Pre	Post	Δ	95% CI	t	df	p	d
Fee (USD)	6.27	4.61	-1.66	[-2.26, -1.06]	5.43	365	1.06e-7	-0.56
Count	548	788	240	[186, 295]	-8.63	350	2.19e-16	0.88
Volume (USD)	1.56e6	3.27e6	1.76e6	[1.42, 1.99] $\times 10^6$	-11.91	314	2.93e-27	1.27

Table 3: Daily averages for cross-chain arbitrage fee, trade count, and volume before and after the Dencun upgrade (March 13, 2024), with mean change Δ , 95% Confidence Intervals (CIs), Welch t , p , and Cohen’s d .

it posts raw data, whereas, e.g., Arbitrum posts compressed call-data [20]—liquidity on its DEXes also increases. Aerodrome’s [4] monthly volume on Base leaps from 229 million USD in February 2024 to 1.39 billion USD in March [21], likely drawing arbitrageurs.

We observe several short-lived spikes in arbitrage volume, typically originating by a handful of token pairs, as illustrated in Figure 7. OMNI—the first token built on LayerZero’s bridging technology [48]—drives activity following its launch on December 22, 2023 but collapses once a CEX, MEXC [44], lists it on December 28. On the other hand, activity on BTC-ETH pairs surges mid-May 2024, after Aerodrome lists tBTC—a bridged Bitcoin token introduced by the Threshold Network [63] which alone accounts for 69.19 % of all BTC-ETH arbitrages. These cases highlight that better interoperability (e.g., via bridgeable tokens) can incentivize traders to engage in cross-chain arbitrage, even for major asset pairs, provided profitable market conditions exist. We present further details on arbitrated token pairs in Appendix D.

Beyond these token-specific bursts, daily cross-chain-arbitrage volume appears to track broader market volatility. Using ETH and BTC as proxies [37], we compute each day’s log high-to-low price ratio and plot it against the daily cross-chain arbitrage volume. Figure 8 reveals moderate yet highly significant Pearson correlations with arbitrage volume (ETH: $r = 0.42$, $p = 5.18 \times 10^{-17}$; BTC: $r = 0.32$, $p = 4.68 \times 10^{-10}$). This pattern suggests that price swings in major assets possibly propagate to other tokens through second-order effects, creating cross-chain arbitrage opportunities.

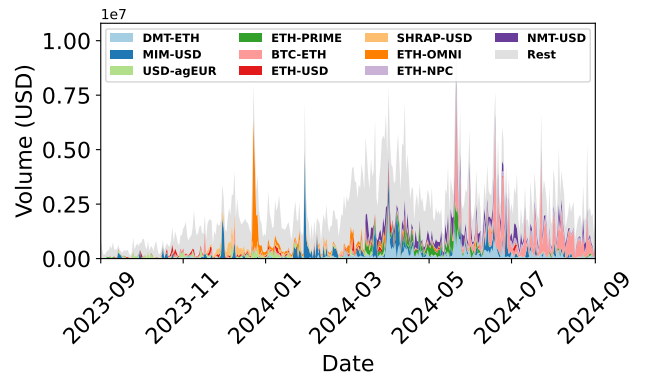


Figure 7: Daily USD volume for the ten token pairs with the highest cumulative arbitrage volume; all other pairs are grouped as “Rest.”

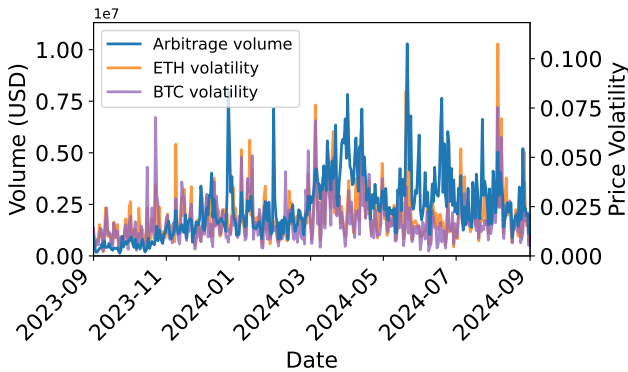


Figure 8: Daily USD cross-chain arbitrage volume against ETH and BTC price volatility.

4.4.2 Execution Methods: Inventory and Bridges. We find that 66.96 % of cross-chain arbitrages rely on pre-positioned inventory across chains rather than transferring traded assets through a bridge. Among bridge-based trades, 71.91 % use multi-chain bridges while the remainder adopt native L1-L2 bridges. Table 4 breaks these figures down by chain-pair category (i.e., L1-L1, L1-L2, L2-L2) and execution method, showing that in every category inventory arbitrage dominates⁶.

A plausible driver of this inventory bias is the time required to complete both legs of the trade. To test that hypothesis, we measure the settlement time—the interval between the two legs of an arbitrage—and plot its distributions in Figure 9. Inventory trades settle fastest, with a 9 s median, followed by multi-chain-bridge trades at 162 s, and native-bridge trades lagging far behind at 1,030 s, yielding an overall 242 s for bridge arbitrage. In other words, bridges impose a considerable *latency cost*. A breakdown confirms that this cost is driven almost entirely by the asset-transfer leg: the interval between the outbound and inbound bridge transactions accounts for 88.23 % of total settlement time in native-bridge arbitrages and 71.16 % in multi-chain-bridge arbitrages. These delays likely explain why traders prefer the recurring cost of holding inventory over the opportunity cost of slow bridging.

We notice that settlement times for native-bridge arbitrages show a bimodal pattern, with a secondary peak near 1,200 s. More than half of these trades (11,314, 50.27 %) occur between Ethereum and Polygon—the most frequently arbitrated chain-pair (see Table 7

⁶Our dataset labels 42 arbitrages between two L2s as “native-bridge” as each trade routes assets through its native bridge to Ethereum before reaching the destination L2.

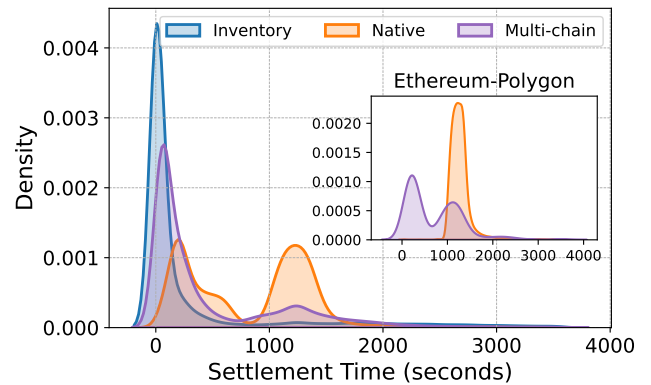


Figure 9: Distribution of settlement times for inventory, native-bridge, and multi-chain-bridge arbitration. The inset highlights Ethereum-Polygon native- and multi-chain-bridge cases.

in Appendix C)—and settle in a median 1,248 s. This latency possibly stems from Polygon’s inherently lengthy checkpoint-based bridge design for securing chain’s consistency and integrity [24]. By contrast, only 687 multi-chain-bridge trades (1.19 %) arbitrage the same pair, despite settling faster (415 s). We discover that token availability appears to be driving this choice. Across the four most-arbitrated L1-L2 pairs that offer native bridges⁷, the asymmetry in bridge use correlates almost perfectly with the share of non-overlapping token pairs (Pearson $r = 0.98$, $p = 0.02$). Ethereum-Polygon sits at the extreme: 94.27 % of bridge-trades use the native one and 97.81 % of token pairs are exclusive to either the native or a multi-chain bridge, but not both. An arbitrageur without inventory must therefore pick whichever bridge supports the desired token—accepting potentially slower settlement (native) or counter-party risk (multi-chain)—constraints that inventory-based strategies avoid.

To examine competition, we look into how often inventory and bridge arbitrages are sent through private mempools—channels that hide transaction details from public (e.g., against frontrunning attacks) and offer features such as revert protection and bundling [32, 43]. However, measuring direct competition is difficult as most rollups lack mempool visibility. We therefore use Ethereum as a proxy since it hosts the highest-volume of activity and offers a public mempool. We observe 35,966 bridge arbitrages, of which 42.81 % adopt private mempools for the swap transaction—just over half of those (52.17 %) also relay the bridge transaction privately—compared to only 26.23 % of 52,298 inventory arbitrages. The heavier reliance on private channels for bridge trades can imply higher competition, which is expected as capital requirements are lower, hence, there is a reduced barrier to entry. This can prompt traders to conceal their strategies and use bundles to ensure atomic execution for the swap and the bridge transaction so that either both succeed or both revert, mitigating partial execution risk.

⁷Ethereum-Scroll and Ethereum-ZKSync are omitted because they contribute negligible arbitrage activity.

Chain-Pair	Inventory		Multi-chain		Native		
	Category	Count	%	Count	%	Count	%
L1-L1		12,533	86.52 %	1,953	13.48 %	0	0.00 %
L1-L2		93,115	65.79 %	25,948	18.33 %	22,464	15.87 %
L2-L2		56,755	65.59 %	29,725	34.36 %	42	0.05 %

Table 4: Distribution of cross-chain arbitrages by chain-pair category and execution method.

We present summary statistics for bridge protocols appearing in our study in Appendix E.

4.4.3 Who Controls Cross-Chain Arbitrage? We observe a long tail of entities—9,064 distinct addresses—engaged in cross-chain arbitrage. Yet activity is highly skewed: Figure 10 shows that the top five addresses execute just over half of all trades, and the top four together command half of the total volume. Most strikingly, one address (0xCA74) alone accounts for more than a third of all volume.

To track concentration dynamics, we plot daily arbitrage activity for the largest traders with at least 1 % of total volume (see Table 11 in Appendix F for detailed statistics). Figure 11 reveals that 0xCA74 becomes progressively more dominant, likely benefiting from the Dencun upgrade: the arbitrageur’s share climbs from 20.3 % before Dencun to 39.7 % afterwards ($t_{340} = -18.6$, $p = 8.14 \times 10^{-54}$). Over the same window it more than doubles its daily trade count (79.4 to 175 , $t_{341} = -17.3$, $p = 9.44 \times 10^{-49}$) and increases its daily volume five-fold (0.35 million to 1.3 million; $t_{238} = -14$, $p = 6.52 \times 10^{-33}$), while its mean fee per trade falls from 10.0 USD to 6.57 USD ($t_{364} = 5.42$, $p = 1.08 \times 10^{-7}$). Full statistics for 0xCA74’s activity before and after Dencun are provided in Table 10 in Appendix F.

We notice that other large actors demonstrate intermittent patterns. For instance, 0x6226—second by trade count—avoids trades involving Ethereum, thereby limiting its volume. By contrast, 74.46 % of 0xCA74’s arbitrages include Ethereum, suggesting that meaningful market dominance demands the capacity to commit large capital to high-volume pairs. This capital barrier sets cross-chain arbitrage apart from single-chain atomic arbitrage, where flash loans eliminate the need for upfront funds.

We find that only three out of the eleven leading arbitrageurs submit trades through MEV smart contracts, and the rest act directly via EOAs. This pattern likely stems from the non-atomic nature of cross-chain arbitrage: a trader cannot embed on-chain logic that both detects an opportunity across multiple chains and executes only if it remains profitable, as is common in single-chain atomic arbitrage. Since no protocol yet guarantees cross-chain atomic execution, traders must build off-chain infrastructure to monitor markets and deploy transactions at the right moment—bearing latency and execution risk. This engineering burden may form a competitive moat and further concentrate the market.

5 Discussion

Cross-chain arbitrage is mainly lucrative to actors who can minimize execution risks—especially latency—and manage inventory across chains. Sequencing control addresses the first challenge: an entity that determines block order on several chains can ensure its multi-chain transaction bundle lands exactly as intended. The second challenge demands trading skill and capital to deploy the right size of inventory on the right chain at the right time.

Together, these requirements create a powerful incentive for *vertical integration*. High-Frequency Trading (HFT) shops and sophisticated MEV searchers (e.g., 0xCA74) can pair their technical know-how with the sequencing leverage of infrastructure operators like centralized rollup sequencers or large staking providers running validators across many Proof-of-Stake (PoS) chains. A similar dynamic is already visible on Ethereum, where several HFT firms

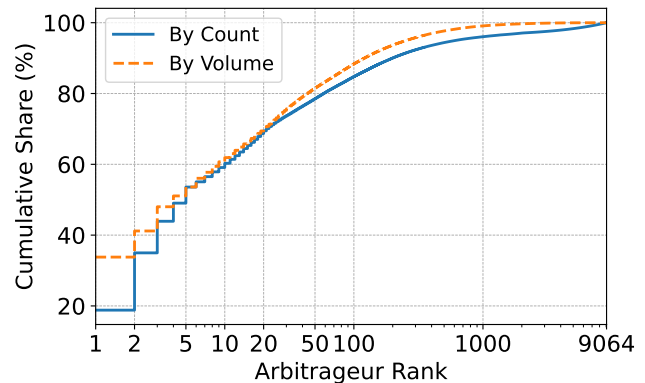


Figure 10: Cumulative distribution of cross-chain arbitrage count (solid blue) and volume (dashed orange) by arbitrageur.

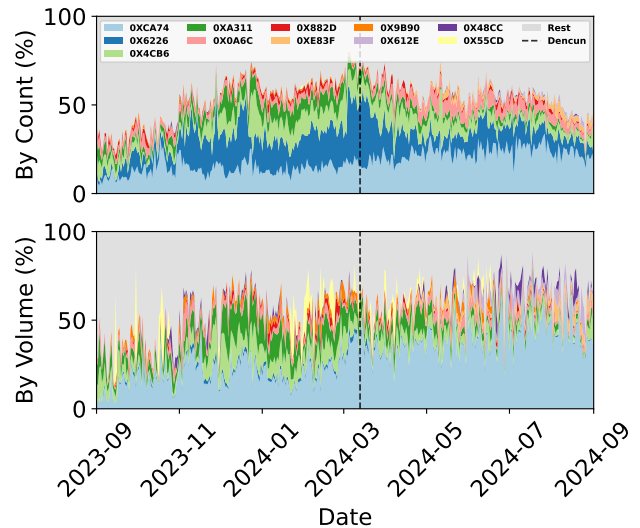


Figure 11: Daily share of cross-chain-arbitrage count (top) and volume (bottom) for addresses with at least 1 % of total volume; all remaining addresses are grouped as “Rest.” The black dashed line marks Ethereum’s Dencun upgrade on March 13, 2024.

now run block builders to execute their strategies with minimal delay [10, 36, 37, 53, 70]. By merging searcher logic with sequencing control, these alliances concentrate both physical infrastructure (clustered in few data-centers) and economic power, creating a feedback loop: *sequencing advantages yield higher MEV, which funds still more sequencing reach*. The result is a small set of centralized gatekeepers, which introduces three systemic hazards: *censorship risk*—economically motivated suppression of competing MEV bundles or compliance with regulatory sanctions [65]; *liveness risk*—a centralized sequencer’s outage or block withholding can stall multiple chains simultaneously; and *finality risk*—multi-chain “time-bandit” re-orgs that rewrite history to extract additional MEV from past blocks [47].

Decentralized block building. To mitigate the risks that follow from MEV-driven economic and infrastructural concentration, block building must be decentralized. On L1s like Ethereum—with already large validator sets—several in-protocol proposals tackle the problem [33, 46, 62, 64]. They seek to break a single block proposer’s monopoly by (i) obliging the proposer to include transactions supplied by other validators (e.g., through inclusion lists [45]), or (ii) assigning multiple proposers to the same slot and merging their blocks deterministically (e.g., by priority-fee order). Outside the protocol, BuilderNet [14] offers a complementary approach: a decentralized network of Trusted Execution Environment (TEE)-backed builders that share the same order flow, so a transaction censored by one builder can still be included by another [14]. Analogous solutions apply to rollups, which now rely on a single sequencer. One path is the based rollup model, which delegates block building to Ethereum validators [25]; this inherits Ethereum’s security and censorship resistance, but also its throughput bottleneck. An alternative is a shared sequencer network such as Espresso [61], which replaces the single rollup sequencer with a decentralized ordering layer: the network only orders transactions—leaving execution to the rollup—thereby reducing unilateral control while maintaining high throughput.

Lowering entry barriers. A complementary way to counteract concentration is to broaden participation in cross-chain arbitrage. When MEV extraction becomes less technically demanding, competition increases and profit margins narrow—as seen in single-chain atomic arbitrage [17]. Reduced margins can weaken the incentive for any infrastructure operator to form an exclusive alliance with an individual MEV searcher.

Lowering barriers requires cutting both inventory overhead and execution latency. *Atomic, instant bridging* across L1s and L2s would let traders move assets inside the same bundle, so they can shift funds just-in-time instead of pre-positioning and continuously rebalancing them. This removes bridge delay and unlocks cross-chain flash loans—a trader can borrow on Chain A, execute leg 1, atomically bridge, execute leg 2 on Chain B, and repay, all in one bundle. A non-atomic variant already exists (borrow on Chain A against collateral, trade on both chains, then bridge back to repay and reclaim the collateral), as illustrated in Figure 12 and detailed in Appendix G. By reducing capital and operational hurdles, atomic bridging widens participation and helps neutralize the centralizing forces discussed above.

6 Related Work

Qin et al. [54] provided one of the first comprehensive quantification of MEV, documenting systematic value extraction through sandwich attacks, liquidations, and DEX arbitrage on Ethereum. Building up on the theoretical work presented by Eskandari et al. [27], Torres et al. [29] presented the first empirical quantification of frontrunning strategies. McLaughlin et al. [41] advanced this understanding by developing an application-agnostic arbitrage detection methodology using standardized ERC-20 transfer events, enabling analysis across a broader range of decentralized exchanges. Torres et al. [30] extended MEV research into L2 solutions by investigating MEV activities across Arbitrum, Optimism, and ZKSync, revealing comparable trading volumes to Ethereum on rollups, albeit with

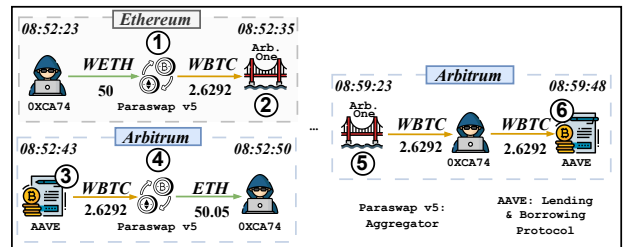


Figure 12: A loan-backed cross-chain arbitrage between Ethereum and Arbitrum. Full transaction details in Appendix G.

significantly lower profits despite reduced costs. Öz et al. [52] provided empirical evidence of MEV extraction on FCFS blockchains. The analysis of non-atomic arbitrage has been advanced by Heimbach et al. [37], who demonstrated that around 25 % of volume on Ethereum’s top five DEXes could be attributed to arbitrage between CEXes and DEXes, revealing substantial centralization among a small group of dominant MEV searchers. Obadia et al. [47] provided the first formal definition of cross-domain MEV by introducing domains as self-contained systems with shared states and showing how cross-domain MEV opportunities incentivize sequencer collusion across chains. McMenamin [42] systematized cross-domain MEV by categorizing extractable value based on extraction methods and value origins while analyzing different protocols’ MEV mitigation capabilities. Mazor et al. [39] examined hypothetical cross-chain arbitrage opportunities between PancakeSwap on Binance Smart Chain and QuickSwap on Polygon, providing insights into the magnitude of extractable arbitrage value and the typical duration of these opportunities. Gogol et al. [35] analyzed price disparities in WETH-USDC trading pairs between Ethereum and major L2 rollups, showing that arbitrage opportunities persisted for multiple blocks with relatively limited profits ranging from 0.03 % to 0.25 % of trading volume. Mazorra et al. [40] provided theoretical foundations by developing an abstract framework for analyzing MEV games across domains, particularly focusing on network characteristics’ influence on strategies and congestion. Finally, Öz et al.’s [53] and Yang et al.’s [70] analyses on block building revealed how private order flow access by select builders leads to market centralization in Ethereum’s block building, highlighting similar centralization risks that could emerge from privileged access to cross-chain MEV opportunities.

7 Conclusion

As trading migrates fully on-chain across multiple networks, cross-chain arbitrage is poised to become DeFi’s primary mechanism for keeping prices aligned across chains. We examine this mechanism with a profit–cost model contrasting inventory- and bridge-based execution, and with a year-long measurement across nine blockchains. The model pinpoints opportunity frequency, bridge time, and token depreciation as the key profitability drivers; empirically, daily volume grew 5.5× over the study window and spiked after Ethereum’s Dencun upgrade. Yet bridges still impose a sizable latency cost: 66.96 % of arbitrages use inventory and settle

in 9 s, whereas bridge trades take 242 s. Activity is concentrated as well—five addresses generate over half of all trades, and one captures nearly 40 % of daily volume post-Dencun. Because this MEV stream rewards vertical integration between searchers and infrastructure operators such as sequencers or staking providers, it risks centralizing sequencing infrastructure and economic power, amplifying censorship, liveness, and finality threats. Decentralizing block building and lowering entry barriers—thereby undercutting exclusive sequencer–searcher deals—are critical countermeasures. We hope these findings inform designs that curb such risks as the ecosystem advances into an ever more multi-chain future.

Acknowledgements

This work is supported by the European Union’s Horizon 2020 research and innovation programme under grant agreement No 952226, project BIG (Enhancing the research and innovation potential of Técnico through Blockchain technologies and design Innovation for social Good). We extend our gratitude to Danut Ilisei, Murad Muradli, and Thomas Wagner for their contributions. We also thank Quintus Kilbourn and Sarah Allen for their valuable feedback.

References

- [1] Aave. 2025. *Aave Documentation*. URL: <https://aave.com/docs>.
- [2] Across Docs. 2025. *FAQ | Across Documentation*. URL: <https://docs.across.to/user-docs/additional-info/faq>.
- [3] Hayden Adams, Noah Zinsmeister, and Dan Robinson. 2020. Uniswap v2 Core.
- [4] Aerodrome. 2025. *Aerodrome Finance*. URL: <https://www.aerodrome.finance/>.
- [5] Allium. 2025. *Allium - Enterprise Blockchain Data Platform*. URL: <https://www.allium.so/>.
- [6] Allium Docs. 2025. *Overview - Allium Documentation Hub*. URL: <https://docs.allium.so/historical-data/prices>.
- [7] Arbitrum Docs. 2025. *A gentle introduction to Arbitrum | Arbitrum Docs*. URL: <https://docs.arbitrum.io/welcome/arbitrum-gentle-introduction>.
- [8] Arbitrum Docs. 2025. *Quickstart: Arbitrum Bridge | Arbitrum Docs*. URL: <https://docs.arbitrum.io/arbitrum-bridge/quickstart>.
- [9] Axelar. 2025. *Exploring Cross-Chain Solutions: how to Bridge Into Arbitrum*. URL: <https://www.axelar.network/blog/arbitrum-bridge>.
- [10] Maryam Bahrami, Pranav Garimidi, and Tim Roughgarden. 2025. Centralization in Block-Building and Proposer-Builder Separation. In *Financial Cryptography and Data Security*, Jeremy Clark and Elaine Shi (Eds.). Springer Nature Switzerland, Cham, 331–349.
- [11] Base Docs. 2025. *Base Docs*. URL: <https://docs.base.org/>.
- [12] Binance. 2025. *Binance Data Collection*. URL: <https://data.binance.vision/>.
- [13] BNB Chain Docs. 2025. *BNB Chain*. URL: <https://docs.bnchain.org>.
- [14] BuilderNet. 2025. Welcome to BuilderNet. <https://builder.net/docs>
- [15] Celer cBridge Docs. 2025. *FAQ | Celer cBridge*. URL: <https://cbridge-docs.celer.network/reference/faq>.
- [16] Vishal Chawla. 2024. Base sees big surge in transactions and users after Dencun upgrade. <https://www.theblock.co/post/283056/base-dencun-transactions-users-surge> Section: Layer 2s and Scaling.
- [17] Eugene Chen, Alex Toberoff, Suraj Srinivasan, and Ankit Chiplunkar. 2023. *A Tale of Two Arbitrages*. <https://frontier.tech/a-tale-of-two-arbitrages> URL: <https://frontier.tech/a-tale-of-two-arbitrages>.
- [18] CoinGecko. 2025. *Top Decentralized Exchanges Ranked by Volume | CoinGecko*. URL: <https://www.coingecko.com/en/exchanges/decentralized>.
- [19] Philip Daian, Steven Goldfeder, Tyler Kell, Yunqi Li, Xueyuan Zhao, Iddo Bentov, Lorenz Breidenbach, and Ari Juels. 2020. Flash Boys 2.0: Frontrunning in Decentralized Exchanges, Miner Extractable Value, and Consensus Instability. In *2020 IEEE Symposium on Security and Privacy (SP)*. 910–927. doi:10.1109/SP40000.2020.00040
- [20] Data Always. 2024. Understanding Minimum Blob Base Fees - Layer 2. <https://ethresear.ch/t/understanding-minimum-blob-base-fees/20489> Section: Layer 2.
- [21] Defillama. 2025. *Aerodrome Volume - Defillama*. URL: <https://defillama.com/dexs/aerodrome>.
- [22] Defillama. 2025. *Ethereum DEX Volume - Defillama*. URL: <https://defillama.com/dexs/chains/ethereum>.
- [23] Polygon Docs. 2025. *PoS - Polygon Knowledge Layer*. URL: <https://docs.polygon.technology/pos/>.
- [24] Polygon Docs. 2025. *PoS to Ethereum - Polygon Knowledge Layer*. URL: <https://docs.polygon.technology/pos/how-to/bridging/ethereum-polygon-matic-to-ethereum>.
- [25] Justin Drake. 2023. Based rollups—superpowers from L1 sequencing - Layer 2. <https://ethresear.ch/t/based-rollups-superpowers-from-l1-sequencing/15016> Section: Layer 2.
- [26] Dune Analytics. 2025. *Dune - Crypto Analytics Powered by Community*. URL: <https://dune.com/home>.
- [27] Shayan Eskandari, Seyedehmahsa Moosavi, and Jeremy Clark. 2019. SoK: Transparent Dishonesty: Front-Running Attacks on Blockchain. In *Financial Cryptography and Data Security - FC 2019 International Workshops, VOTING and WTS, St. Kitts, St. Kitts and Nevis, February 18–22, 2019, Revised Selected Papers (Lecture Notes in Computer Science, Vol. 11599)*, Andrea Bracciali, Jeremy Clark, Federico Pintore, Peter B. Rønne, and Massimiliano Sala (Eds.). Springer, 170–189.
- [28] Ethereum.org. 2025. *Cancun - Deneb (Dencun) FAQ*. URL: <https://ethereum.org/en/roadmap/dencun/>.
- [29] Christof Ferreira Torres, Ramiro Camino, and Radu State. 2021. Frontrunner Jones and the Raiders of the Dark Forest: An Empirical Study of Frontrunning on the Ethereum Blockchain. In *30th USENIX Security Symposium, USENIX Security 2021, August 11–13, 2021*, Michael D. Bailey and Rachel Greenstadt (Eds.). USENIX Association, 1343–1359.
- [30] Christof Ferreira Torres, Albin Mamuti, Ben Weintraub, Cristina Nita-Rotaru, and Shweta Shinde. 2024. Rolling in the Shadows: Analyzing the Extraction of MEV Across Layer-2 Rollups. In *Proceedings of the 2024 on ACM SIGSAC Conference on Computer and Communications Security (Salt Lake City, UT, USA) (CCS '24)*. Association for Computing Machinery, New York, NY, USA, 2591–2605. doi:10.1145/3658644.3690259
- [31] Flashbots. 2024. *Mempool Dumpster*. URL: <https://github.com/flashbots/mempool-dumpster>.
- [32] Flashbots Docs. 2025. *MEV Protection - Block MEV With Flashbots Protect RPC*. URL: <https://docs.flashbots.net/flashbots-protect/overview>.
- [33] Elijah Fox, Mallesh M. Pai, and Max Resnick. 2023. Censorship Resistance in On-Chain Auctions. In *5th Conference on Advances in Financial Technologies (AFT 2023) (Leibniz International Proceedings in Informatics (LIPIcs), Vol. 282)*, Joseph Bonneau and S. Matthew Weinberg (Eds.). Schloss Dagstuhl – Leibniz-Zentrum für Informatik, Dagstuhl, Germany, 19:1–19:20. doi:10.4230/LIPIcs.AFT.2023.19
- [34] Robin Fritsch, Maria Inês Silva, Akaki Mamageishvili, Benjamin Livshits, and Edward W. Felten. 2024. MEV Capture Through Time-Advantaged Arbitrage. arXiv:2410.10797 [cs.DC] <https://arxiv.org/abs/2410.10797>
- [35] Krzysztof Gogol, Johnnathan Messias, Deborah Miori, Claudio Tessone, and Benjamin Livshits. 2024. Cross-Rollup MEV: Non-Atomic Arbitrage Across L2 Blockchains. <http://arxiv.org/abs/2406.02172> arXiv:2406.02172
- [36] Tivas Gupta, Mallesh M. Pai, and Max Resnick. 2023. The Centralizing Effects of Private Order Flow on Proposer-Builder Separation. In *5th Conference on Advances in Financial Technologies (AFT 2023) (Leibniz International Proceedings in Informatics (LIPIcs), Vol. 282)*, Joseph Bonneau and S. Matthew Weinberg (Eds.). Schloss Dagstuhl – Leibniz-Zentrum für Informatik, Dagstuhl, Germany, 20:1–20:15. doi:10.4230/LIPIcs.AFT.2023.20
- [37] Lioba Heimbach, Vabuk Pahari, and Eric Schertenleib. 2024. Non-Atomic Arbitrage in Decentralized Finance. In *2024 IEEE Symposium on Security and Privacy (SP)*. IEEE Computer Society, Los Alamitos, CA, USA, 224–224. doi:10.1109/SP54263.2024.00256
- [38] LayerZero Docs. 2025. *LayerZero Documentation | LayerZero*. URL: <https://docs.layerzero.network/v2>.
- [39] Ori Mazor and Ori Rottenstreich. 2023. An Empirical Study of Cross-chain Arbitrage in Decentralized Exchanges. <https://eprint.iacr.org/2023/1898> Publication info: Published elsewhere. Minor revision. International Conference on Communication Systems and Networks (COMSNETS) 2024.
- [40] Bruno Mazorra, Michael Reynolds, and Vanesa Daza. 2022. Price of MEV: Towards a Game Theoretical Approach to MEV. *Proceedings of the 2022 ACM CCS Workshop on Decentralized Finance and Security* (2022). <https://api.semanticscholar.org/CorpusID:251903953>
- [41] Robert McLaughlin, Christopher Kruegel, and Giovanni Vigna. 2023. A large scale study of the Ethereum arbitrage ecosystem. In *Proceedings of the 32nd USENIX Conference on Security Symposium (Anaheim, CA, USA) (SEC '23)*. USENIX Association, USA, Article 185, 18 pages.
- [42] Conor McMenamin. 2023. SoK: Cross-Domain MEV. arXiv:2308.04159 [cs.CR] <https://arxiv.org/abs/2308.04159>
- [43] MEV Blocker. 2025. *Mev Blocker - The best MEV protection under the sun*. URL: <https://cow.fi/mev-blocker>.
- [44] MEXC. 2025. *About MEXC | User-friendly Cryptocurrency Service Provider*. URL: <https://www.mexc.com/about>.
- [45] Michael Neuder, Vitalik Buterin, Francesco D’Amato, Terence Tsao, Potuz, and Manav Gupta. 2023. EIP-7547: Inclusion lists. <https://eips.ethereum.org/EIPS/eip-7547>. Ethereum Improvement Proposals, no. 7547.

- [46] Mike Neuder and Max Resnick. 2024. Concurrent Block Proposers in Ethereum - Proof-of-Stake / Block proposer. <https://ethresear.ch/t/concurrent-block-proposers-in-ethereum/18777>
- [47] Alexandre Obadia, Alejo Salles, Lakshman Sankar, Tarun Chitra, Vaibhav Chellani, and Philip Daian. 2021. Unity is Strength: A Formalization of Cross-Domain Maximal Extractable Value. arXiv:2112.01472 [cs.CR] <https://arxiv.org/abs/2112.01472>
- [48] OmniCat. 2025. *OmniCat*. URL: <https://omnicat.wtf>.
- [49] Optimism Docs. 2025. *Using the Standard Bridge* / Optimism Docs. URL: <https://docs.optimism.io/builders/app-developers/bridging/standard-bridge>.
- [50] Optimism Docs. 2025. *Welcome to the Optimism Docs.* URL: <https://docs.optimism.io/>.
- [51] Burak Öz, Benjamin Kraner, Nicolò Vallarano, Bingle Stegmann Kruger, Florian Matthes, and Claudio Juan Tessone. 2023. Time Moves Faster When There is Nothing You Anticipate: The Role of Time in MEV Rewards. In *Proceedings of the 2023 Workshop on Decentralized Finance and Security* (Copenhagen, Denmark) (*DeFi '23*). Association for Computing Machinery, New York, NY, USA, 1–8. doi:10.1145/3605768.3623563
- [52] Burak Öz, Filip Rezabek, Jonas Gebele, Felix Hoops, and Florian Matthes. 2024. A Study of MEV Extraction Techniques on a First-Come-First-Served Blockchain. In *Proceedings of the 39th ACM/SIGAPP Symposium on Applied Computing* (Avila, Spain) (*SAC '24*). Association for Computing Machinery, New York, NY, USA, 288–297. doi:10.1145/3605098.3635990
- [53] Burak Öz, Danning Sui, Thomas Thiery, and Florian Matthes. 2024. Who Wins Ethereum Block Building Auctions and Why?. In *6th Conference on Advances in Financial Technologies (AFT 2024)* (*Leibniz International Proceedings in Informatics (LIPIcs)*, Vol. 316). Rainer Böhme and Lucianna Kiffer (Eds.). Schloss Dagstuhl – Leibniz-Zentrum für Informatik, Dagstuhl, Germany, 22:1–22:25. doi:10.4230/LIPIcs.AFT.2024.22
- [54] Kaihua Qin, Liyi Zhou, and Arthur Gervais. 2022. Quantifying blockchain extractable value: How dark is the forest?. In *2022 IEEE Symposium on Security and Privacy (SP)*. IEEE, 198–214.
- [55] Team Rocket, Maofan Yin, Kevin Sekniqi, Robbert van Renesse, and Emin Gün Sirer. 2020. Scalable and Probabilistic Leaderless BFT Consensus through Metastability. arXiv:1906.08936 [cs.DC] <https://arxiv.org/abs/1906.08936>
- [56] Caspar Schwarz-Schilling, Fahad Saleh, Thomas Thiery, Jennifer Pan, Nihar Shah, and Barnabé Monnot. 2023. Time Is Money: Strategic Timing Games in Proof-Of-Stake Protocols. In *5th Conference on Advances in Financial Technologies (AFT 2023)* (*Leibniz International Proceedings in Informatics (LIPIcs)*, Vol. 282). Joseph Bonneau and S. Matthew Weinberg (Eds.). Schloss Dagstuhl – Leibniz-Zentrum für Informatik, Dagstuhl, Germany, 30:1–30:17. doi:10.4230/LIPIcs.AFT.2023.30
- [57] Scroll. 2024. Scroll White Paper. <https://scroll.io/files/whitepaper.pdf>. Accessed: 2025-06-17.
- [58] Scroll Docs. 2025. *Bridge / Scroll Documentation*. URL: <https://docs.scroll.io/en/user-guide/bridge>.
- [59] Superbridge Docs. 2025. *What is bridging?* / Superbridge Docs. URL: <https://docs.superbridge.app/what-is-bridging>.
- [60] Synapse Docs. 2025. *Transaction Support FAQ* / Synapse Docs. URL: <https://docs.synapseprotocol.com/docs/Support/Transaction-Support>.
- [61] Espresso Systems. 2024. The Espresso Sequencer. <https://hackmd.io/@EspressoSystems/EspressoSequencer>
- [62] Thomas Thiery, Francesco D’amatto, and Julian Ma. 2024. Fork-Choice enforced Inclusion Lists (FOCIL): A simple committee-based inclusion list proposal - Proof-of-Stake / Block proposer. <https://ethresear.ch/t/fork-choice-enforced-inclusion-lists-focil-a-simple-committee-based-inclusion-list-proposal/19870>
- [63] Threshold Network Docs. 2025. *What is the Threshold Network?* / Threshold Docs. URL: <https://docs.threshold.network/>.
- [64] Sarish Wadhwa, Julian Ma, Thomas Thiery, Barnabe Monnot, Luca Zanolini, Fan Zhang, and Kartik Nayak. 2025. AUCIL: An Inclusion List Design for Rational Parties. Cryptology ePrint Archive, Paper 2025/194. <https://eprint.iacr.org/2025/194>
- [65] Anton Wahrstätter, Jens Ernstberger, Aviv Yaish, Liyi Zhou, Kaihua Qin, Taro Tsuchiya, Sebastian Steinhorst, Davor Svetinovic, Nicolas Christin, Mikolaj Barczentewicz, and Arthur Gervais. 2023. Blockchain Censorship. <https://arxiv.org/abs/2305.18545v2>
- [66] Ye Wang, Yan Chen, Haotian Wu, Liyi Zhou, Shuguang Deng, and Roger Wattenhofer. 2022. Cyclic Arbitrage in Decentralized Exchanges. In *Companion Proceedings of the Web Conference 2022* (Virtual Event, Lyon, France) (*WWW '22*). Association for Computing Machinery, New York, NY, USA, 12–19. doi:10.1145/3487553.3524201
- [67] winnsterx. 2025. *searcherbuilder.pics*. URL: https://github.com/winnsterx/searcherbuilder.pics/blob/main/labels/non_mev_contracts.py.
- [68] Gavin Wood et al. 2014. Ethereum: A secure decentralised generalised transaction ledger. *Ethereum project yellow paper* 151, 2014 (2014), 1–32.
- [69] Wormhole Docs. 2025. *Native Token Transfers Rate Limiting* / Wormhole Docs. URL: <https://wormhole.com/docs/build/contract-integrations/native-token-transfers/configuration/rate-limiting>.
- [70] Sen Yang, Kartik Nayak, and Fan Zhang. 2025. Decentralization of Ethereum’s Builder Market . In *2025 IEEE Symposium on Security and Privacy (SP)*. IEEE Computer Society, Los Alamitos, CA, USA, 1512–1530. doi:10.1109/SP6157.2025.00157
- [71] Sen Yang, Fan Zhang, Ken Huang, Xi Chen, Youwei Yang, and Feng Zhu. 2024. SoK: MEV Countermeasures. In *Proceedings of the Workshop on Decentralized Finance and Security* (Salt Lake City, UT, USA) (*Defi '24*). Association for Computing Machinery, New York, NY, USA, 21–30. doi:10.1145/3689931.3694911
- [72] ZKSync Docs. 2025. *Bridges - ZKSync Docs*. URL: <https://docs.zksync.io/zksync-era/ecosystem/bridges>.
- [73] ZKSync Docs. 2025. *ZKSync Docs*. URL: <https://docs.zksync.io/>.

A Cost of Inventory with Bounded Liquidity

The formulae for the cost of liquidity calculation can be adapted to the case of bounded liquidity in the second market, as we sketch next:

Suppose the second market has bounded liquidity and is also operated as a CPMM with reserves \tilde{R}_t^A and \tilde{R}_t^B . A good approximation of a CPMM is that of quadratic trading cost. More specifically, define the trading cost of a CPMM to be the difference in exchanged tokens between a perfectly liquid market and the CPMM,

$$\tilde{C}_t(x) := Q_t x - \frac{\tilde{R}_t^A x}{\tilde{R}_t^B + x} = \frac{Q_t x (\tilde{R}_t^B + x) - \tilde{R}_t^A x}{\tilde{R}_t^B + x} = \frac{Q_t x^2}{\tilde{R}_t^B + x}.$$

Then for small trade sizes relative to the total liquidity in the pool, we can approximate trading cost by

$$\tilde{C}_t(x) \approx \frac{Q_t x^2}{\tilde{R}_t^B}.$$

The cost of inventory has now a cost term:

$$\begin{aligned} C(I) &= E_0 \left[\int_0^\tau \frac{Q_t}{\tilde{R}_t^B} (dI_t)^2 - \int_0^\tau I_t dQ_t \right] \\ &= E_0 \left[\int_0^\tau \frac{Q_t}{\tilde{R}_t^B} \sigma^2 \left(\frac{\partial I_t}{\partial Q_t} \right)^2 dt - \int_0^\tau I_t dQ_t \right]. \end{aligned}$$

For the case of reserves

$$R_t^B = \frac{Q_0^k}{Q_t^k} R_0^B$$

and a constant multiply of reserves in the second AMM, $\tilde{R}_t^A = \phi R_A$ and $\tilde{R}_t^B = \phi R_B$, we obtain for example:

$$\begin{aligned} \frac{C(I)}{E_0[Q_t I_t]} &= \frac{\lambda + (1-k)(\frac{1}{2}k\sigma^2 - \mu)}{\lambda R_0^A} E_0 \left[\int_0^\tau \frac{Q_t}{\phi R_t^B} \left(\frac{k R_t^B}{Q_t} \right)^2 \sigma^2 dt \right] - \frac{\mu}{\lambda} \\ &= \frac{\lambda + (1-k)(\frac{1}{2}k\sigma^2 - \mu)}{\lambda R_0^A} E_0 \left[\int_0^\tau \frac{k^2}{\phi Q_t} R_t^B \sigma^2 dt \right] - \frac{\mu}{\lambda} \\ &= \frac{1-k}{1+k} \frac{(\lambda/(1-k) - \mu + \frac{1}{2}k\sigma^2)k^2\sigma^2}{\phi \lambda Q_0^2 (\lambda/(k+1) + \mu - \frac{1}{2}\sigma^2(k+2))} - \frac{\mu}{\lambda}. \end{aligned}$$

In the case of $k = 0$, we obtain:

$$-\frac{\mu}{\lambda}$$

and in the case of $k = 1/2$ we obtain:

$$\frac{1}{3} \frac{(2\lambda - \mu + \frac{1}{4}\sigma^2)\frac{1}{4}\sigma^2}{\phi \lambda Q_0^2 (\frac{3}{2}\lambda + \mu - 5\sigma^2)} - \frac{\mu}{\lambda}$$

B Cross-Chain Arbitrage Examples

We now breakdown real-world examples of an inventory arbitrage and a bridge arbitrage.

B.1 Case Study: Inventory Arbitrage

Table 5 summarizes a real-world example of an inventory arbitrage—see Figure 1a for an illustration. The arbitrageur first swaps 0.9 WETH for 1,034,616.49 OMNI on Base at 12:25:51 AM. On Arbitrum, they swap 1,034,616.49 OMNI for close to 1 WETH, earning approximately 198.95 USD in profit after deducting transaction fees. The entire arbitrage gets completed in 27 s. Post-arbitrage, the arbitrageur rebalances their inventory by transferring 1,034,616.49 OMNI from Base to Arbitrum using the LayerZero bridge⁸.

Transaction Hash	Blockchain	From	To	Type	Time
0xeb546...37f7c	Base	0x4cb...3d9	0x6bd...891	Swap	12:25:51 AM
0xffeb...aa7aa	Arbitrum	0x4cb...3d9	0x1b0...506	Swap	12:26:18 AM

Table 5: Breakdown of an inventory arbitrage between Base and Arbitrum.

B.2 Case Study: Bridge Arbitrage

Table 6 summarizes a real-world example of a bridge arbitrage—see Figure 1b for an illustration. The arbitrageur initially swaps 20,000 USDT for 2,692,596.48 VOW on Ethereum at 11:13:11 AM. Following this, they approve DBridge to transfer VOW tokens and deposit 2,692,590 VOW 60 s later. The arbitrageur receives 2,692,590 VOW on Binance Smart Chain at 11:19:10 AM and, 12 s later, swaps 2,692,593.08 VOW for 134,889.18 Binance-Peg BSC-USD, earning around 114,688.38 USD in profit after transaction fees. The entire arbitrage takes over 6 minutes to complete.

Transaction Hash	Blockchain	From	To	Type	Time
0x59237...61999	Ethereum	0xe6b...532	0x111...a65	Swap	11:13:11 AM
0x64fa3...46aa8	Ethereum	0xe6b...532	0xa7c...44d	Bridge	11:14:11 AM
0x73307...591ec	BSC*	0xe6b...532	0xa7c...44d	Bridge	11:19:10 AM
0x101d0...cea91	BSC*	0xe6b...532	0x111...a65	Swap	11:19:22 AM

* Binance Smart Chain.

Table 6: Breakdown of a bridge arbitrage between Ethereum and BSC.

C Blockchain Pairs

Table 7 summarizes the cross-chain arbitrage metrics for all blockchain pairs in our study.

D Tokens

Table 8 reports summary statistics for the ten token pairs with the largest cumulative arbitrage volume; together they account for 43.05 % of total volume. The remaining 1,858 pairs share the other 56.95 %.

⁸Rebalance transactions: Base 0x11e...dcf, Arbitrum 0x2b8...7dca.

E Bridges

Table 9 summarizes the usage metrics of native and multi-chain bridges for cross-chain arbitrages, excluding those used in less than 0.1 % of all bridge arbitrage. The *Cost Ratio* column shows, for each bridge, the share of total transaction fees attributable to the bridge leg relative to the aggregate fees of the entire arbitrage.

F Arbitrageurs

0xCA74 Activity. Table 10 reports the statistics for the cross-chain arbitrage activity of the arbitrageur 0xCA74, before and after the Dencun upgrade.

Summary Statistics. Table 11 summarizes the cross-chain arbitrage metrics for arbitrageurs executing $\geq 1\%$ of the total trade volume; together they account for 63.01 % of total volume. The remaining 9,053 traders conduct the other 37.99 %.

G Case Study: Loan-Backed Arbitrage

When an arbitrageur lacks pre-positioned inventory, the usual fallback is to bridge assets across chains—incurring delay and execution risk. A faster workaround is to *borrow* the required tokens from a lending protocol, execute the arbitrage instantaneously as though the inventory were already in place, and then bridge the proceeds back to repay the loan. This loan-backed method replicates inventory arbitrage without the upfront capital commitment, at the cost of paying loan fees and taking temporary price risk during the bridge leg.

Figure 12 shows a real-world loan-backed arbitrage executed by 0xCA74 between Ethereum and Arbitrum. The process unfolds as follows:

- (1) 0xCA74 initially swaps 50 WETH for 2.629 WBTC on Ethereum (0xf9d...08a).
- (2) The WBTC is bridged to Arbitrum in the next block (0x452...903).
- (3) 8 s later, 0xCA74 takes a loan for 2.629 WBTC using Aave [1] (0xf7e...eff).
- (4) The WBTC is then swapped back to ETH, earning 0.5 ETH and completing the arbitrage (0xdd4...72f).
- (5) The bridged WBTC arrives on Arbitrum around 7 minutes after the arbitrage is completed (0x701...1bf).
- (6) Finally, 0xCA74 transfers the bridged WBTC to AAVE to close the loan, concluding the strategy (0x798...935).

Chain Pair	Total [USD]		Average [USD]		Count	Execution Method [%]			Settlement Time [s]		
	Volume	Profit	Volume	Profit		Inventory	Multi-chain	Native	25th	50th	75th
ARB-ETH	243,611,503.97	1,640,759.86	11,757.31	79.19	20,720	50.77	29.05	20.17	12.00	105.00	369.00
BASE-ETH	136,809,634.57	1,671,060.39	6,709.64	81.95	20,390	54.70	20.76	24.55	14.00	194.00	318.00
BSC-ETH	106,614,309.82	1,447,488.64	7,359.82	99.92	14,486	86.52	13.48	0.00	9.00	97.00	285.00
ETH-POL	103,521,335.22	1,473,049.96	3,760.17	53.51	27,531	56.41	2.50	41.10	188.50	1,251.00	1,888.00
ARB-BASE	43,308,426.15	276,184.86	2,556.43	16.30	16,941	68.18	31.82	0.00	2.00	28.00	130.00
BASE-OP	42,010,397.87	232,645.08	2,375.75	13.16	17,683	57.44	42.54	0.02	10.00	66.00	218.00
ARB-BSC	34,239,480.03	303,282.66	1,331.81	11.80	25,709	65.55	34.45	0.00	2.00	7.00	74.00
ARB-POL	31,883,971.14	167,111.54	2,310.77	12.11	13,798	82.54	17.44	0.01	5.00	8.00	190.00
ARB-OP	25,277,935.69	133,137.93	2,019.65	10.64	12,516	60.17	39.83	0.00	19.00	89.00	403.00
AVA-ETH	15,546,710.75	174,235.31	8,152.44	91.37	1,907	83.69	16.31	0.00	9.00	17.00	247.50
ETH-OP	13,165,677.85	233,166.07	4,246.99	75.21	3,100	28.48	8.52	63.00	84.00	102.00	154.00
ARB-SCROLL	12,323,983.83	8,504.15	10,877.30	7.51	1,133	99.47	0.53	0.00	3.00	5.00	18.00
ARB-AVA	11,337,989.28	299,109.72	1,483.25	39.13	7,644	42.61	57.39	0.00	9.00	38.00	81.00
BASE-POL	9,875,258.02	78,817.79	1,316.17	10.50	7,503	81.01	18.75	0.24	6.00	117.00	416.50
BSC-POL	9,109,320.4	183,862.16	376.82	7.61	24,174	93.34	6.65	0.00	4.00	6.00	61.00
BASE-BSC	8,374,722.52	94,455.39	1,024.06	11.55	8,178	72.57	27.43	0.00	3.00	53.00	201.75
AVA-BSC	6,586,964.25	74,915.78	792.66	9.02	8,310	86.75	13.25	0.00	3.00	5.00	47.00
ETH-SCROLL	3,674,739.91	3,374.46	34,343.36	31.54	107	71.03	24.30	4.67	20.50	27.00	369.50
OP-POL	3,424,785.64	21,126.36	1,105.48	6.82	3,098	45.80	53.58	0.61	168.00	382.00	807.75
AVA-POL	2,111,453.94	35,268.49	693.42	11.58	3,045	84.60	15.40	0.00	7.00	41.00	264.00
BSC-OP	1,530,040.17	54,319.71	1,289.00	45.76	1,187	57.20	42.80	0.00	7.00	105.00	642.00
OP-SCROLL	1,166,887.32	1,450.7	10,705.39	13.31	109	100.00	0.00	0.00	3.00	7.00	20.00
AVA-BASE	1,065,823.0	20,944.82	666.97	13.11	1,598	61.45	38.55	0.00	6.00	46.00	113.00
AVA-OP	540,371.31	7,904.1	1,382.02	20.22	391	40.15	59.85	0.00	58.50	138.00	562.00
ARB-ZKSYNC	456,054.82	1,193.76	1,646.41	4.31	277	36.82	63.18	0.00	23.00	176.00	380.00
POL-SCROLL	429,752.1	779.99	9,767.09	17.73	44	97.73	2.27	0.00	15.00	26.00	283.50
ETH-ZKSYNC	138,119.84	164.84	6,005.21	7.17	23	30.43	43.48	26.09	353.00	657.00	1,259.50
BSC-ZKSYNC	129,435.05	8,571.36	1,307.42	86.58	99	31.31	68.69	0.00	108.00	154.00	383.50
BASE-SCROLL	116,708.87	246.81	2,714.16	5.74	43	74.42	25.58	0.00	18.00	26.00	102.50
BASE-ZKSYNC	115,157.55	3,615.37	170.10	5.34	677	33.83	66.17	0.00	154.00	301.00	575.00
BSC-SCROLL	71,601.75	1,053.71	778.28	11.45	92	84.78	15.22	0.00	121.00	172.00	213.75
OP-ZKSYNC	58,086.12	1.11	3,227.01	0.06	18	66.67	33.33	0.00	10.00	17.50	171.50
SCROLL-ZKSYNC	15,231.91	-2.73	3,807.98	-0.68	4	100.00	0.00	0.00	11.50	12.00	14.75

Table 7: Cross-chain arbitrage statistics for all chain-pairs in our dataset.

Token Pair	Total [USD]		Average [USD]		Count
	Volume	Profit	Volume	Profit	
BTC-ETH	94,481,876.03	115,151.06	31,368.48	38.23	3,012
MIM-USD	53,992,514.62	113,038.14	43,263.23	90.58	1,248
NMT-USD	47,672,408.90	486,996.21	28,822.50	294.44	1,654
DMT-ETH	46,490,116.88	306,793.02	12,269.76	80.97	3,789
ETH-OMNI	32,253,198.96	403,176.99	2,627.98	32.85	12,273
ETH-PRIME	30,026,851.42	160,867.88	19,334.74	103.59	1,553
USD-ageEUR	19,521,861.60	219,876.53	5,894.28	66.39	3,312
ETH-NPC	18,818,700.27	147,817.12	5,162.88	40.55	3,645
SHRAP-USD	15,426,515.75	112,919.70	5,352.71	39.18	2,882
ETH-USD	15,223,335.86	27,860.14	5,137.81	9.40	2,963

Table 8: Summary statistics for the ten token pairs with the highest cumulative arbitrage volume.

Bridge	Count	Averages		Cost Ratio [%]	
		Duration [s]	Cost [USD]	Bridge Fee/Tx Fee	
LayerZero	39,536	165.56	1.64	26.86	
Native	22,506	739.40	4.91	30.29	
Wormhole	8,566	990.68	2.03	29.63	
Axelar	3,212	1,364.93	0.45	21.51	
Celer	2,815	281.21	0.66	24.55	
Across	2,639	269.99	0.24	18.83	
Synapse	472	391.28	0.94	22.59	
Stargate	315	133.66	0.93	26.07	

Table 9: Summary statistics for bridge protocols used in ≥ 0.1 % of bridge-based cross-chain arbitrages.

Metric	Pre	Post	Δ	95% CI	t	df	p	d
Fee (USD)	10	6.57	-3.44	[-4.68, -2.19]	5.42	364	1.08e-7	-0.56
Count	79.4	175	95.4	[84.5, 106]	-17.3	341	9.44e-49	1.78
Volume (USD)	3.57e5	1.3e6	9.38e5	[0.8, 1.07] × 10 ⁶	-14	238	6.52e-33	1.52
Volume (%)	20.3%	39.7%	19.3%	[17.3, 21.4]%	-18.6	340	8.14e-54	1.96

Table 10: Arbitrageur 0xCAT4's daily averages for cross-chain arbitrage fee, trade count, and volume before and after the Dencun upgrade (March 13, 2024), with mean change Δ, 95% CIs, Welch t, p, and Cohen's d.

Arbitrageur		Totals [USD]		Averages [USD]		Count	Execution Method [%]		Settlement Time [s]		
Address	Type	Volume	Profit	Volume	Profit		Inventory	Bridge	25th	50th	75th
0xCA74	EOA	293,534,534.50	2,043,570.41	6,433.77	44.79	45,624	68.00	32.00	6.00	64.00	528.00
0xA311 [†]	SC	64,089,695.72	578,432.65	5,156.46	46.54	12,429	50.90	49.10	3.00	27.00	58.00
0x4CB6	EOA	59,428,683.84	400,555.17	2,745.10	18.50	21,649	73.90	26.10	2.00	6.00	38.00
0x0A6C [†]	SC	26,573,871.45	282,973.40	2,414.49	25.71	11,006	21.69	78.31	134.00	228.00	575.00
0x9B90	EOA	21,928,158.44	241,282.77	14,407.46	158.53	1,522	64.91	35.09	9.00	13.00	60.00
0x55CD	EOA	21,378,753.99	12,090.77	194,352.31	109.92	110	19.09	80.91	89.00	168.00	281.75
0x612E	EOA	14,721,732.01	101,750.09	23,554.77	162.80	625	100.00	0.00	79.00	117.00	138.00
0x48CC	EOA	14,495,989.50	10,637.47	35,270.05	25.88	411	100.00	0.00	17.00	21.00	25.00
0x882D	SC	11,252,232.57	189,184.18	3,436.85	57.78	3,274	53.12	46.88	1,138.00	1,345.00	2,299.00
0xE83F	EOA	10,276,396.37	81,094.31	4,336.03	34.22	2,370	45.02	54.98	82.00	232.00	936.25
0x6226	EOA	9,664,552.84	141,303.17	246.36	3.60	39,229	99.99	0.01	2.00	4.00	6.00

[†]EOA identified via its SC.

Table 11: Cross-chain arbitrage metrics for arbitrageurs with $\geq 1\%$ of the total trade volume. EOA - Externally Owned Account, SC - Smart Contract.